Tertiary sequence of deformation in a thin-skinned/thick-skinned collision belt: The Zagros Folded Belt (Fars, Iran)

F. Mouthereau, J. Tensi, N. Bellahsen, O. Lacombe, T. de Boisgrollier, S. Kargar

Tertiary sequence of deformation in a thin-skinned/thick-skinned collision belt: The Zagros Folded Belt (Fars, Iran)

F. Mouthereau,[1] J. Tensi,[1] N. Bellahsen,[1] O. Lacombe,[1] T. De Boisgrollier,[1] and S. Kargar[2]

Received 3 January 2007; revised 14 June 2007; accepted 5 July 2007; published 27 September 2007.

[1] We describe how thin-skinned/thick-skinned deformation in the Zagros Folded Belt interacted in time and space. Homogeneous fold wavelengths (15.8 ± 5.3 km), tectono-sedimentary evidence for simultaneous fold growth in the past 5.5 ± 2.5 Ma, drainage network organization, and homogeneous peak differential stresses (40 ± 15 MPa) together point to buckling as the dominant process responsible for cover folding. Basin analysis reveals that basement inversion occurred ~20 Ma ago as the Arabia/Eurasian plate convergence reduced and accumulation of Neogene siliciclastics in foreland basin started. By 10 Ma, ongoing contraction occurred by underplating of Arabian crustal units beneath the Iranian plate. This process represents 75% of the total shortening. It is not before 5 Ma that the Zagros foreland was incorporated into the southward propagating basement thrust wedge. Folds rejuvenated by 3–2 Ma because of uplift driven by basement shortening and erosion. Since then, folds grew at 0.3—0.6 mm/yr and forced the rivers to flow axially. A total shortening of 65–78 km (16–19%) is estimated across the Zagros. This corresponds to shortening rates of 6.5–8 km/Ma consistent with current geodetic surveys. We point out that although thin-skinned deformation in the sedimentary cover may be important, basement-involved shortening should not be neglected as it requires far less shortening. Moreover, for such foreland folded belts involving basement shortening, underplating may be an efficient process accommodating a significant part of the plate convergence. **Citation:** Mouthereau, F., J. Tensi, N. Bellahsen, O. Lacombe, T. de Boisgrollier, and S. Kargar (2007), Tertiary sequence of deformation in a thin-skinned/thick-skinned collision belt: The Zagros Folded Belt (Fars, Iran), *Tectonics*, *26*, TC5006, doi:10.1029/2007TC002098.

1. Introduction

[2] In an attempt at illustrating the structure and kinematics of foreland fold-and-thrust belts, the most popular model, thin-skinned in style, considers it as the product of continuous subduction of the lower plate basement beneath the upper plate. There are several limitations for using such a thin-skinned deformation model for collisional settings as it assumes that a significant part of the total plate convergence might be accommodated at the front, by rocks accretion above a sole thrust at shallow crustal levels and hence neglects intraplate basement thickening, giving rise to unrealistically high cover shortening. The alternative thick-skinned interpretation is supported by our current knowledge on the rheology of the continental crust: it is buoyant and rheologically stratified, including a ductile lower crust, which allows for decoupling the upper crust from the mantle. Moreover, the development of foreland fold-and-thrust belts over rifted continental margin likely promotes reverse-reactivation/inversion of preorogenic basement normal faults. Such basement-involved deformation simply highlights plate coupling in collisional settings and requires far less shortening than equivalent thin-skinned models do.

[3] Numerous examples exist of external fold-and-thrust belts in which basement is known to be involved in the compressional deformation such as the Andes [*Zapata and Allmendinger*, 1996; *Cristallini and Ramos*, 2000], the northern Apennines [*Coward et al.*, 1999; *Butler et al.*, 2004], Taiwan [*Lee et al.*, 2002; *Mouthereau and Lacombe*, 2006], the Alps [*Meyer et al.*, 1994; *Lacombe and Mouthereau*, 2002; *Rostein and Schaming*, 2004], the Zagros [*Sherkati and Letouzey*, 2004; *Molinaro et al.*, 2005]. In spite of increasing evidence supporting the coexistence of both thin-skinned and thick-skinned interpretation at belt fronts, the interplay in time and space of both deformations has received, to date, little attention. However, our understanding of the overall kinematic evolution of mountain belts is dependent on our understanding of how and when contraction of the basement is transferred up-section to the cover sequence folding.

[4] The Zagros folded belt offers a unique opportunity to examine such interactions. The presence of a thick and weak salt-bearing formation at the base of the sedimentary cover and fold geometry has led for years to interpret the structural style in the Zagros Folded Belt in thin-skinned style [*Davis and Engelder*, 1985]. Since crystalline basement is generally not exposed in forelands, the recognition of underlying basement-involved deformation is usually indirect [e.g., *Lacombe and Mouthereau*, 2002]. In the northwest of the Zagros Folded Belt, basement-involved shortening was required for balancing the differential uplift between adjacent synclines [*Blanc et al.*, 2003; *Sherkati and Letouzey*, 2004]. This is probably the present-day crustal deformation patterns including seismotectonic studies that

[1] Laboratoire Tectonique, Université Pierre et Marie Curie, UMR 7072, Paris, France.
[2] Geological Survey of Iran, Tehran, Iran.

0278-7407/07/2007TC002098$12.00

provide the more reliable evidence for thick-skinned deformation [*Jackson*, 1980; *Ni and Barazangi*, 1986; *Berberian*, 1995]. It is no doubt that both structural styles currently coexist in the Zagros Folded Belt, but to first order this is the growth of a thrust wedge including basement-involved deformation that is mechanically required to maintain the current topography [*Mouthereau et al.*, 2006].

[5] Our goal in this paper is to examine how thin-skinned deformation and thick-skinned deformation in the Zagros Folded Belt have interacted in time and space since the Middle Miocene. To this aim we provide a new crustal-scale section across the Central Fars area of the Zagros Folded Belt. We use isopach maps to assess the large-scale tectonically induced movements, which have controlled the sedimentation in the Zagros foreland basin. Unconformities reported from fieldwork within the synorogenic Neogene strata of the synclinal valleys offer direct constraints regarding the inception and the growth of cover folding. In order to decipher the last Quaternary increment of shortening, rates of folding and sequence of deformation between thick-skinned and thin-skinned mode, we examine folds geomorphology and associated drainage networks. In the absence of currently reliable stratigraphic ages of the synorogenic continental deposits, age constraints are brought by the extrapolation of synorogenic accumulation rates in the Zagros Folded Belt to the observed thickness of strata with unconstrained ages. These data are used to give preliminary indicative estimates for fold uplift rates averaged over the past 3–2 Ma, which have been poorly constrained so far. With the aim at offering a viable mechanical explanation of the sequence of deformation, we discuss the possibility that cover folding may result primarily from the growth of buckling instabilities rather than fault-related folding. On the basis of the restored regional crustal-scale section and our results on the sequence of deformation we draw a forward scenario of the Tertiary evolution of the Zagros Folded Belt from basin inversion, inception of thin-skinned fold growth to the current basement-involved thrusting. All these results finally place constraints on the topographic evolution of the Zagros orogeny and potential Neogene climatic forcing in the framework of the Arabia/Eurasia plate convergence.

2. Central Fars: Geological Background

[6] The Zagros Mountains form a broad orogenic domain in Iran, approximately 2000 km long, in front of the Turkish-Iranian plateau (Figure 1). The mountain belt results from the ongoing accommodation of the convergence between the rifted continental margin of the Arabian plate and the Iranian continental blocks following the closure of the Neo-Tethys ocean during the Tertiary [*Stocklin*, 1968; *Koop and Stoneley*, 1982]. The present-day convergence between Arabia and Eurasia is 2–3 cm/yr [*Vernant et al.*, 2004] in the N–S direction and is assumed to be unchanged since at least 10 Ma [*McQuarrie et al.*, 2003]. The collision suture zone is outlined, along the Main Zagros Thrust (MZT), by a complex of ophiolitic rocks, deep-water radiolarites and eruptive rocks interpreted as remnants of the obducted Neo-Tethyan ocean or one of its derivative (e.g., back-arc or fore-arc crust) [*Stoneley*, 1990; *Ziegler*, 2001]. The tectono-metamorphic belt of Sanandaj-Sirjan North of the MZT represents the former active margin of the Iranian microplate (Figure 1). To the South, the Imbricate Zone (or High Zagros) and the Zagros Folded Belt (ZFB) form a large external folded domain within the rifted Arabian continental margin.

[7] In this paper we focus on the Central Fars province of the Zagros Folded Belt (Figures 1 and 2). It is a 200-km-wide arcuate folded belt, south of the High Zagros Fault, characterized by periodic, symmetrical and open concentric folds with axial lengths often greater than 100 km. The ZFB results from the folding of a thick pile of sedimentary rocks up to 12 km [*Stocklin*, 1968; *Falcon*, 1974; *Colman-Sadd*, 1978] including Paleozoic, Mesozoic strata and Cenozoic synorogenic deposits (Figures 2 and 3). The exceptional geomorphic expression of folds, the so-called "whaleback" shape of folds, is related to the presence, within the upper part of the folded pile, of resistant carbonates belonging to the Asmari Formation, Oligo-Miocene in age. Noticeably, the topographic elevation of the crest of anticlines above local base levels is remarkably uniform.

3. Crustal-Scale Cross Section of the Zagros (Central Fars)

3.1. Subsurface Constraints on the Crustal Structure of the Zagros Folded Belt and Internal Domains

[8] In order to examine the sequence of deformation and to estimate finite shortening in both the cover and the basement we have constructed a crustal-scale balanced section across the Zagros Folded Belt, the High Zagros and the Sanandaj-Sirjan Zone (Figures 2 and 4). Surface geology was constrained by field studies, Landsat images and geological maps from the National Iranian Oil Company (1:1,000,000 and 1:250,000 scale maps). Subsurface constraints in the ZFB were provided by the thickness distribution of Paleozoic, Mesozoic and Cenozoic strata from available isopachs and basement isobaths derived from aeromagnetic surveys [*Motiei*, 1993].

[9] Our cross section extends northward into the Sanandaj-Sirjan area. However, it was beyond our objectives to study the structure of the SSZ, so we treat this folded domain as a coherent assemblage of tectono-metamorphic units belonging to the upper Iranian plate. The suture zone, which is represented by the ophiolites of Neyriz, is exposed just 50 km east of the studied section (Figure 2). This ophiolitic complex represents a klippen of allochthonous radiolarites, peridotites and exotic masses of Mesozoic carbonate overthrusted onto the continental margin in the Late Cretaceous (Figure 3). The oceanic basin has now disappeared but we expect that ophiolitic units are present below the SSZ units. This is suggested by the geometry of the Moho provided by recent geophysical studies and receiver functions revealing that the Arabian crust and possibly the oceanic crust have been underplated below the MZT [*Hatzfeld et al.*, 2003; *Paul et al.*, 2006]. The

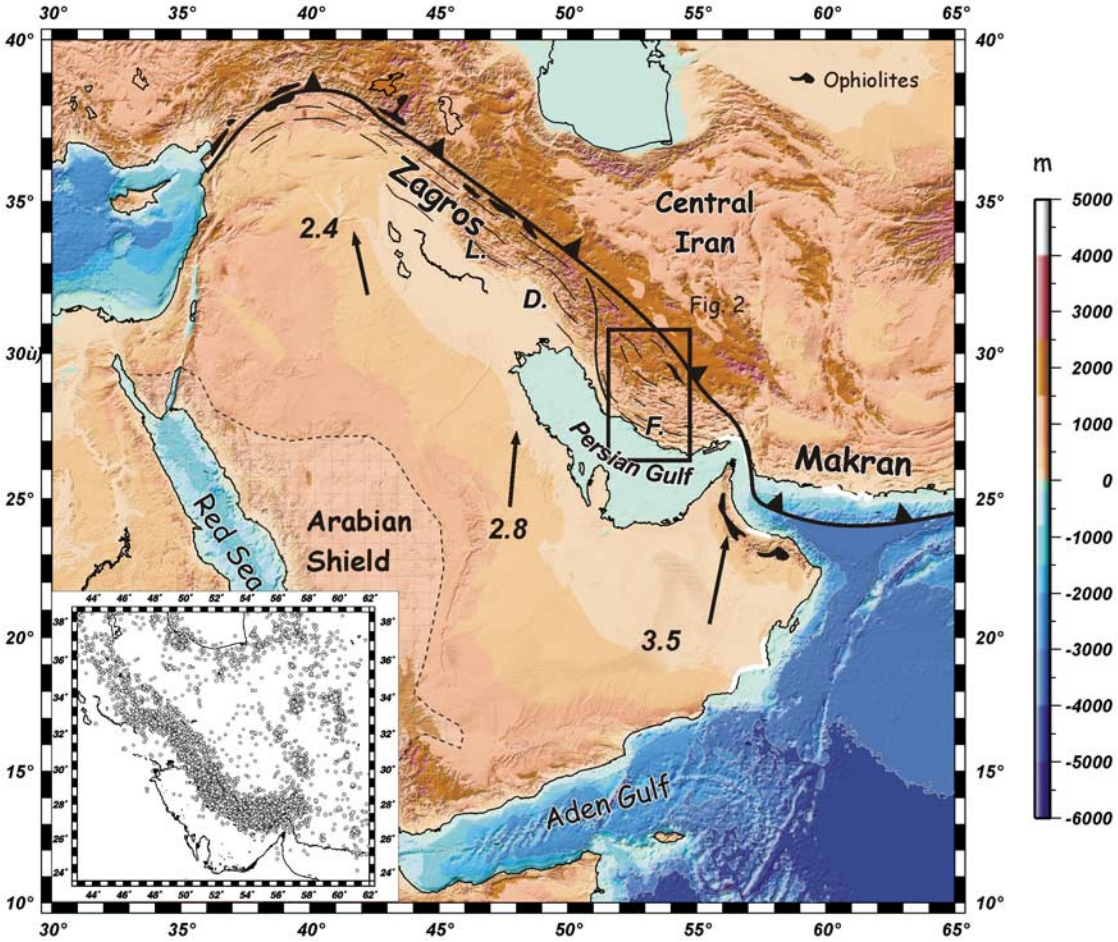

Figure 1. Zagros Folded Belt in the framework of the Arabia/Eurasia plate convergence. Black arrows indicate the present-day convergence of the Arabian plate with respect to stable Eurasia [*De Mets et al.*, 1994]. It predicts a present-day convergence of ~3 ± 0.5 cm/yr oriented N–S on average at the front of the Zagros Mountains. The studied area of the Central Fars province is indicated by a black quadrangle. The suture zone is outlined by remnants of ophiolitic series and the Main Zagros Thrust (MZT). The inset in the lower left shows seismicity in the Zagros for earthquakes with focal depths shallower than 35 km and magnitudes $2.4 < m_b < 7.4$ (data issued from ISC and CMT catalogs, years 1965–2003). Capital letters L, D, and F for Lorestan, Dezful, and Fars areas, respectively.

depth of the mechanical lithosphere is set to 100 km in slightly stretched areas of the Arabian continental margin, which corresponds to the depth of the 700°–800°C isotherm [*Burov and Diament*, 1995].

3.2. Superimposed Thin-Skinned and Thick-Skinned Deformation

[10] Figure 4 clearly shows that deep-seated thick-skinned deformation is overlain by thin-skinned deformation mode at a shallower crustal level. The preservation of layer area required in balancing is solved by filling the core of anticlines by the 2-km-thick ductile Hormuz Formation and/or by basement culminations outlining the thick-skinned deformation style.

[11] Numerous features of the ZFB including low topographic slopes [*Talbot and Alavi*, 1996], symmetrical anticlines and the lack of clear fold vergence have been referred to as the expression of a brittle thin-skinned wedge

Figure 2. Geological map of the Fars based on a compilation of geological 1:250,000 and 1:100,000 scale maps from the *National Iranian Oil Company* [1977]. The Imbricate Zone (High Zagros) north of the High Zagros Fault is characterized by the lack of Oligo-Miocene deposits which contrast with the Zagros Folded Belt to the south. The anticlines and the major transverse strike-slip fault zone mentioned in the present are depicted. The thick black solid line corresponds to the location of the crustal-scale section of Figure 4. Two compressive focal mechanisms after [*Talebian and Jackson*, 2004] located to the north of the Surmeh Fault have been used to constrain the geometry at depth of the Surmeh basement thrust.

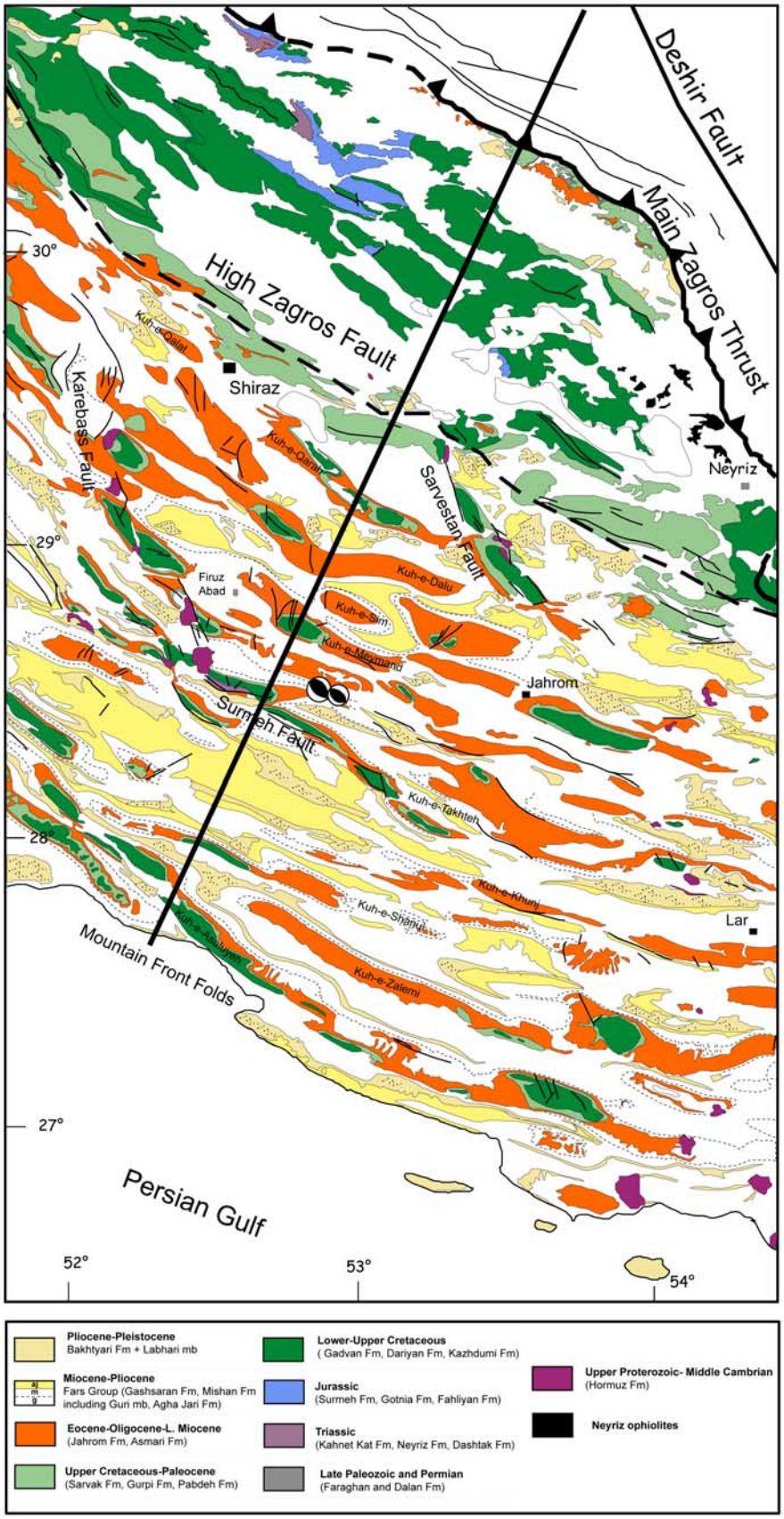
Deshir Fault
Main Zagros Thrust
High Zagros Fault
Karebass Fault
Sarveslan Fault
Surmeh Fault
Mountain Front Folds
Persian Gulf
Shiraz
Neyriz
Jahrom
Lar
Firuz Abad
Kuh-e-Dinar
Kuh-e-Daliu
Kuh-e-Sim
Kuh-e-Meymand
Kuh-e-Takhteh
Kuh-e-Khuny
Kuh-e-Shanul
Kuh-e-Asmari
Kuh-e-Zalemi
30°
29°
28°
27°
52°
53°
54°
Pliocene-Pleistocene
Bakhtyari Fm + Labhari mb
Miocene-Pliocene
Fars Group (Gashsaran Fm, Mishan Fm including Guri mb, Agha Jari Fm)
Eocene-Oligocene-L. Miocene
(Jahrom Fm, Asmari Fm)
Upper Cretaceous-Paleocene
(Sarvak Fm, Gurpi Fm, Pabdeh Fm)
Lower-Upper Cretaceous
(Gadvan Fm, Dariyan Fm, Kazhdumi Fm)
Jurassic
(Surmeh Fm, Gotnia Fm, Fahliyan Fm)
Triassic
(Kahnet Kat Fm, Neyriz Fm, Dashtak Fm)
Late Paleozoic and Permian
(Faraghan and Dalan Fm)
Upper Proterozoic- Middle Cambrian
(Hormuz Fm)
Neyriz ophiolites

Figure 2

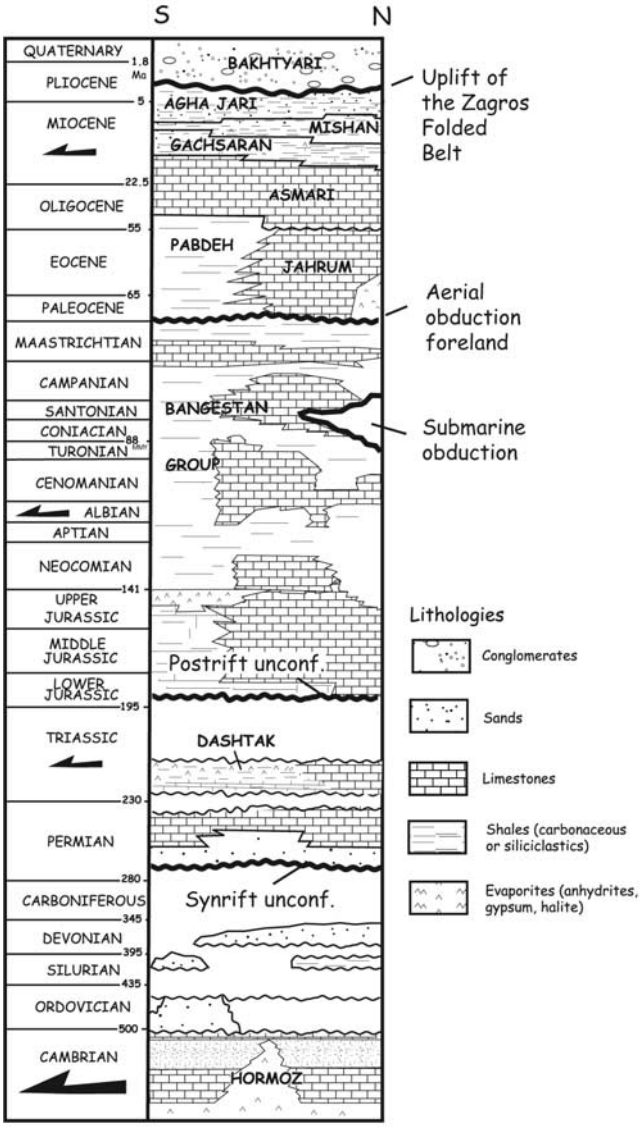

Figure 3. Simplified chronostratigraphic chart and lithologies encountered in the Central Fars after *Motiei* [1993]. The basal décollement (largest black arrow) of the folded cover lies within the Eo-Cambrian salts of the Hormuz formation. Other smaller black arrows refer to second-order and shallower layers that may act as potential detachment levels in the Zagros Folded Belt. Major unconformities are depicted to emphasize the main periods of tectonic activity experienced by the Arabian margin since rifting to collision and uplift of the Zagros.

overlying a ductile décollement [*Davis and Engelder*, 1985]. The structural styles of the ZFB in the Central Fars, however, differs from other salt-based wedges like the Jura folded belt [*Sommaruga*, 1999] or the Salt Ranges in Pakistan [*Jaumé and Lillie*, 1988] in several points. First, there is a lack of unambiguous evidence for thrust-related folding (Figures 2 and 4). Second, the ratio of the maximum folds amplitude (500–1000 m [see *Mouthereau et al.*, 2006, Figure 8]) to the fold wavelength (15.8 ± 5.3 km; see Figure 5) is remarkably constant throughout the belt indicating insignificant deformation gradient. The lack of increasing shortening toward the rear of the ZFB is in agreement with the nearly homogeneous Mio-Pliocene peak differential stresses values (40 ± 15 MPa), which were determined from analyses of calcite twinning across the Simply Folded Belt in synfolding veins and host rocks [*Lacombe et al.*, 2007]. This suggests that cover folding might be primarily linked to pure-shear deformation and buckling of the sedimentary rocks rather then brittle tectonic wedging as suggested by recent studies [*Schmalholz et al.*, 2002; *Mouthereau et al.*, 2007]. Furthermore, the space problem related to the projection to depth of concentric folds may be solved assuming that part of the cover shortening is taken up by plastic and viscous internal deformation such as pressure solution or calcite twinning [*Lacombe et al.*, 2007; *Mouthereau et al.*, 2007]. The quasiperfect sinusoidal shape of cover folds appears to be essentially superimposed onto the larger-scale regional topographic slope originated in the basement. As a result, instead of the common feature of a weak basal décollement dipping toward the hinterland, the Hormuz décollement regionally dips toward the foreland at the top of the basement wedge.

[12] The way basement deforms is however significantly different since faulting seems to be an important, but not unique, mechanism accommodating contraction in the basement as shown by the seismicity [*Berberian*, 1995; *Talebian and Jackson*, 2004; *Tatar et al.*, 2004]. The observation of the lack of basement seismogenic strain rate with respect to cover geodetic strain rate however provides evidence for longer-term ductile and aseismic deformation in the crust [*Jackson and McKenzie*, 1988; *Masson et al.*, 2004]. The location and the dip of major basement-involved thrusts in Figure 4 are provided by the study of historical earthquakes and current focal mechanisms reported in this area [*Ambraseys and Melville*, 1982; *Berberian*, 1995]. For instance, the dip of the Surmeh thrust was constrained by focal mechanisms of two earthquakes with magnitudes M_w higher than 4.6 [*Talebian and Jackson*, 2004]. Both of them occurred at depth shallower than 15 km and are consistent with reverse motion along the moderately dipping Surmeh thrust. The depth at which decoupling between the upper brittle crust and the underlying ductile lower crust likely occurs can be used as an additional constraint to infer the position of the low-angle ductile reverse shear zone; the depth of decoupling lies between 33 and 39 km given a Moho depth at 45 km [*Mouthereau et al.*, 2006]. Beneath the Imbricate Zone, a third basement-involved thrust is proposed in order to explain the exposure of Mesozoic rocks in the absence of cover thrusting.

[13] The displacement across active basement faults has been indirectly estimated by vertical offset of local base levels. The total vertical movement within the basement, which is accommodated by reverse faults, is consistent with the cumulated regional topographic elevation of 2500 m (equivalent to a topographic slope of 0.5° on average). By

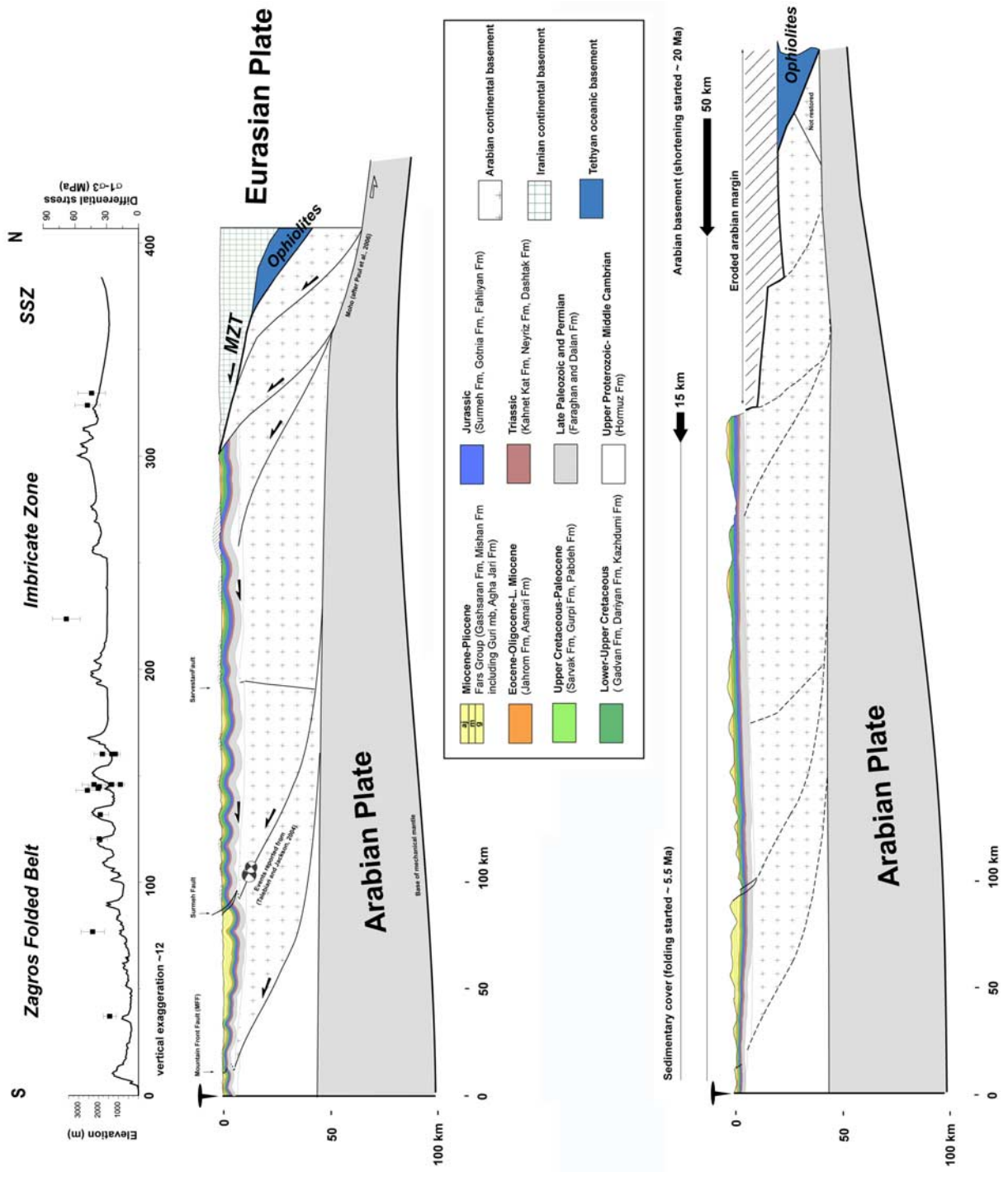
S
Zagros Folded Belt
Imbricate Zone
SSZ
N
Elevation (m)
Differential stress σ1-σ3 (MPa)
vertical exaggeration ~12
Mountain Front Fault (MFF)
Surmeh Fault
Sarvestan Fault
MZT
Ophiolites
Eurasian Plate
Arabian Plate
Moho (after Paul et al., 2006)
Base of mechanical mantle
Miocene-Pliocene
Fars Group (Gashsaran Fm, Mishan Fm including Guri mb, Agha Jari Fm)
Eocene-Oligocene-L. Miocene
(Jahrom Fm, Asmari Fm)
Upper Cretaceous-Paleocene
(Sarvak Fm, Gurpi Fm, Pabdeh Fm)
Lower-Upper Cretaceous
(Gadvan Fm, Dariyan Fm, Kazhdumi Fm)
Jurassic
(Surmeh Fm, Gotnia Fm, Fahliyan Fm)
Triassic
(Kahnet Kat Fm, Neyriz Fm, Dashtak Fm)
Late Paleozoic and Permian
(Faraghan and Dalan Fm)
Upper Proterozoic- Middle Cambrian
(Hormuz Fm)
Arabian continental basement
Iranian continental basement
Tethyan oceanic basement
Sedimentary cover (folding started ~ 5.5 Ma)
15 km
Arabian basement (shortening started ~ 20 Ma)
50 km
Eroded arabian margin
Ophiolites
Not restored
Arabian Plate
0
50
100 km

Figure 4

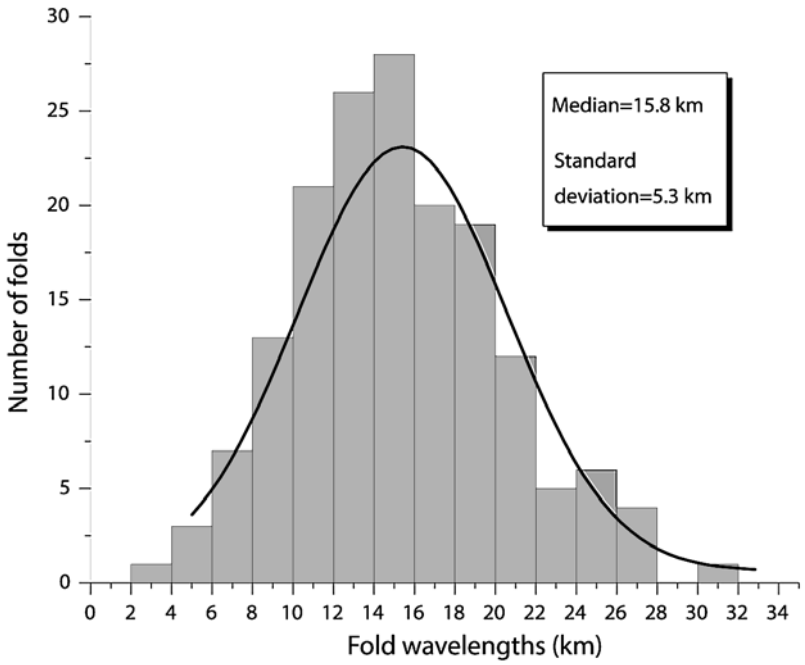

Figure 5. Distribution of fold wavelengths measured for 149 anticlines (modified after *Mouthereau et al.* [2007]). Fold widths have been estimated as the distance between two adjacent synclines independently from the stratigraphy of the folded strata. The diagram shows the calculated statistical Gaussian distribution. It reveals that Zagros folds have a dominant wavelength of 15.8 ± 5.3 km.

means of horizontal contraction, and assumption on faults dip, the observed uplift corresponds to shortening of about 15 km. Excess of outward propagation along basement thrusts with respect to the overlying cover allows for differential plastic deformation possibly accommodated by triangle zones within the Hormuz Salt (Figure 4).

[14] A noticeable difference from previous cross sections in the Fars [*McQuarrie*, 2004] is the lack of thrusts associated with cover folding. If microscale and mesoscale faulting does occur in the sedimentary cover [*Lacombe et al.*, 2006], at larger scale, evidence for fold-related thrusting is generally lacking in the field and not supported by the depth of earthquakes mostly located in the basement [e.g., *Talebian and Jackson*, 2004]. The sedimentary cover is however cut by major thrusts exactly where seismogenic fault zones are reported in the basement such as above the Mountain Front Fault, the Surmeh-Karebass and Sabz-Pushan transverse fault zones. Another evidence is that spacing for fold-related thrusts imposed by the dominant folds wavelength (Figure 5) is too small for fitting internal friction angle in classical brittle thin-skinned wedge [*Mouthereau et al.*, 2006]. We do not exclude, however, as shortening increases and fold limbs rotate that thrusting occurred to accommodate plastic strain in folds hinges.

3.3. Role of Intermediate Cover Décollement Levels

[15] Another difference in regard to the Dezful-Izeh area [*Sherkati and Letouzey*, 2004] and the Bandar-Abbas area [*Molinaro et al.*, 2005] is that intermediate cover décollement levels are lacking in our section. Though the well-known Neogene evaporites-bearing layers of the Gashsaran Formation are present in the southern Fars, no layer-parallel shear has been reported, so it is probably not acting as an intermediate detachment in the studied area. Moreover, the

Figure 4. Crustal-scale section of the Zagros Folded Belt. Subsurface constraints in the ZFB were provided by the thickness distribution of Paleozoic, Mesozoic, and Cenozoic strata from available isopachs and basement isobaths derived from aeromagnetic surveys [*Motiei*, 1993]. The Sanandaj-Sirjan Zone (SSZ) is shown as a coherent assemblage of tectono-metamorphic units belonging to the upper Iranian plate. The currently inactive suture zone is represented by the ophiolites of Neyriz. Tectonic underplating beneath the SSZ area is suggested by the geometry of the Moho provided by recent geophysical studies and receiver functions [*Hatzfeld et al.*, 2003; *Paul et al.*, 2006]. The depth of the mechanical lithosphere is set to 100 km in the unbended and slightly stretched areas of the Arabian continental margin, i.e., at the Mountain Front, which corresponds to the depth of the 700°–800°C isotherm [*Burov and Diament*, 1995]. Exaggerated topography and differential stresses that derived from calcite twinning analyses are shown above [*Lacombe et al.*, 2007].

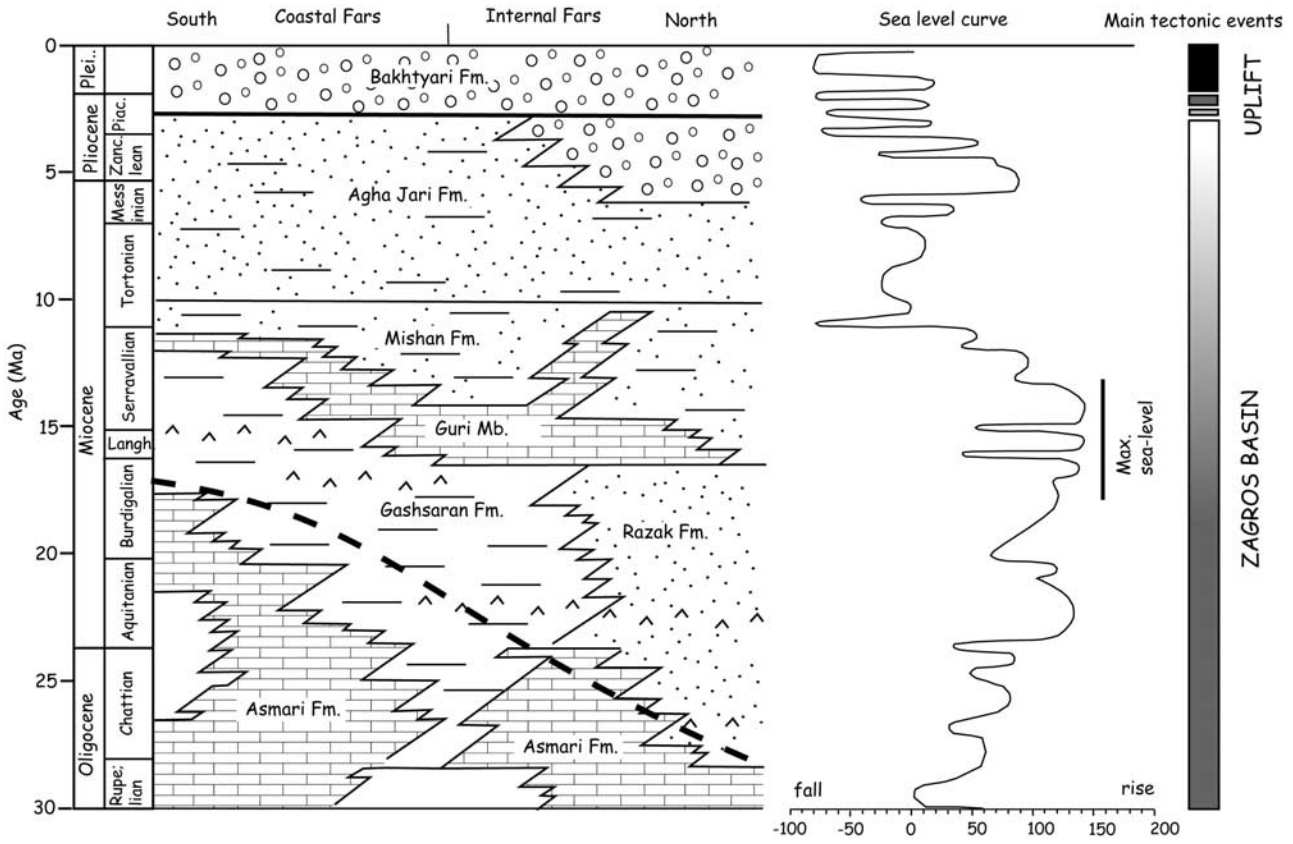

Figure 6. Stratigraphy of the Oligocene and Neogene strata contemporaneous with the Zagros orogeny (modified after *James and Wynd* [1965]). Black dashed line outlines the southward onlap progressive in time of the shallowing-upward synorogenic deposition (Razak-Gashsaran Formation) onto the carbonates of the Asmari Formation in the context of flexural basin development. Eustatic sea level curve is after *Haq et al.* [1987].

existence of an intermediate potential detachment, for example, the evaporitic horizon of the Triassic Dashtak Formation (Figure 3), would lead to uniform reduction of the wavelengths of folding, which is not observed either in the field or based on subsurface data [*Sherkati et al.*, 2005; *Oveisi et al.*, 2007]. Intermediate detachment layers appear of second-order importance to explain the observed dominant wavelength, the style of folding being primarily controlled by the thickness of a single competent unit and the decoupling above a single basal décollement layer lying in the Hormuz Formation (Figure 5).

3.4. Restoration and Estimates of Crustal Shortening

[16] Across both the Zagros Folded Belt and the Imbricate Zone, we estimate only ~15 km (~5%) of horizontal shortening taken up in both the cover and the basement. In our interpretation, restoration of cover thrusts show clear structural relationships with ancient NW–SE-trending extensional faults inherited from the Tethyan rifting.

[17] The geometry of the Moho deduced from the tomography [*Paul et al.*, 2006] shows that the Arabian margin was tectonically thickened and underplated beneath the Main Zagros Thrust. To account for this observation, thrust sheets including basement and cover units are likely to be root beneath the MZT. These units presumably correspond to former half-grabens accommodating the thinning of the passive continental margin, secondarily inverted when orogenic contraction began. We estimate 50 km of shortening related to underplating of Arabian crust beneath the Iranian plate. In this scenario, the current position of the ophiolitic units is found 50 km north of the MZT beneath the SSZ. The thickness and nature of the sedimentary cover deposited above the continental rise and oceanic crust, together with syn-obduction strata deposited in the footwall of the overthrusted oceanic crust is however unknown. Indeed, they were probably removed by erosion and/or underplated beneath the ophiolitic units.

[18] In order to account for penetrative deformation we consider that possibly up to 30% of plastic-viscous internal deformation may occur in agreement with some estimates obtained elsewhere [*Sans et al.*, 2003]. The section thus accounts for a total shortening of 65 km (16%) or 78 km (19%) considering 30% of additional shortening. These

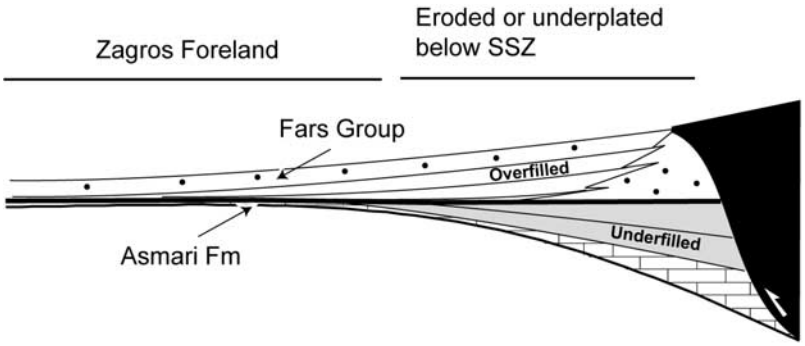

Figure 7. Position of the Fars Group in the schematically reconstructed Neogene Zagros foreland basin before folding and uplift. Only distal parts of the basin are preserved in the current configuration of the ZFB as shown by the prograding sequences of the Fars Group, which correspond to the overfilled stage of the foreland basin. The proximal parts of the basin of the underfilled stage were eroded or underthrusted below the Sanandaj-Sirjan units of the upper Iranian plate.

values are close to another estimate of 17% proposed in the same region [*McQuarrie*, 2004].

4. Foreland Neogene Sequences: Evidence for Early Miocene Margin Inversion

[19] To evaluate the possibility for margin inversion during the early stages of the collision, we examine the relation in space between thickening/thinning of the synorogenic siliciclastic deposits and the current position of large-scale basement faulting within the basin. Sedimentological data, isopach maps based on a compilation performed by *Motiei* [1993] and stratigraphic constraints provided by *James and Wynd* [1965] and *Homke et al.* [2004] are combined along with information from fieldwork.

[20] Foreland basins form by the flexure of the lithosphere in front of advancing thrust-fold belts or under a combination of orogenic and subcrustal loads [e.g., *Watts*, 2001]. The inception of foreland deposition is often found in association with an unconformity that is attributed to the rapid subsidence and drowning of precollisional margin sequences. As the collision migrates, the synorogenic siliciclastic foreland sequences are characterized by onlaps of the margin sequences and a deepening-upward sequence above the foreland unconformity.

[21] In the Zagros Basin, foreland sequences of Miocene ages are represented by a thick regressive siliciclastic sequence (up to 3000 m), namely, the Fars Group lying above the well-developed carbonate platform of the Asmari Formation (Figures 2 and 6). Figure 6 shows that the initiation of foreland siliclastics deposition is delayed toward the foreland: the onset of clastics deposition is Chattian (~28 Ma) in the northern Fars whereas it is Burdigalian (~20–16 Ma) near the Persian Gulf. The prograding sequences of the Fars Group likely correspond to the typical overfilled stage often reported in foreland basins [*Sinclair*, 1997]. The inception of foreland transgressive sequences above margin strata is however not clearly identified from the sedimentary patterns (Figure 7) though the carbonates of the Asmari Formation may represent part of this initial transgressive sequence. We challenge that most of the fining-upward foreland sequences have been deposited northward then eroded and/or buried below the MZT.

[22] Isopachs maps of Figure 8 show an inhomogeneous pattern of deposition. The thickness of the Fars Group is maximum to the north owing to plate flexure. Second-order NW–SE-trending depocenters reveal a complex pattern of subsidence in relation with tectonic inheritance and basement block faulting in the Arabian margin. The deposition of the Fars Group in the foreland domain coincides with a significant increase in accumulation rates up to 182 m/Ma over the past 12 Ma (Figure 9).

4.1. Early Miocene: Gashsaran/Razak Formations

[23] The Lower Miocene is represented by the Gashsaran and the Razak formations in the southern and the northern parts of the studied area, respectively. They form a prograding sequence overlying the Asmari limestones (Figures 6 and 7). Though fieldwork did not bring evidence for unconformities at the base of these series, the Gashsaran Formation and the lower Mishan Formation are locally missing above the Asmari carbonates, near the coast of the Persian Gulf, on the southern limb of the Asaluyeh anticline [*Mouthereau et al.*, 2006].

[24] In the northern Zagros, the Razak Formation consists of 900-m-thick red shales with nodular anhydrites, typical of intertidal to supratidal sabkhas environments [*Tucker*, 2005]. The local abundance of red siltstones and sandstones beds with megaripples shows that the sedimentation is controlled by clastic sediment supplies (Figure 10a). Southward, the thickness of the Gashsaran/Razak formations reduces to 600 m above a paleo-bathymetric high. Near Firuz Abad (labeled F in Figure 8), the thickness of the Gashsaran/Razak Formation increases to 900 m. These deposits are characterized by deeper intertidal and infratidal environment represented by shallow-marine bioclastic wackestones locally named Champeh Member (Figure 10b).

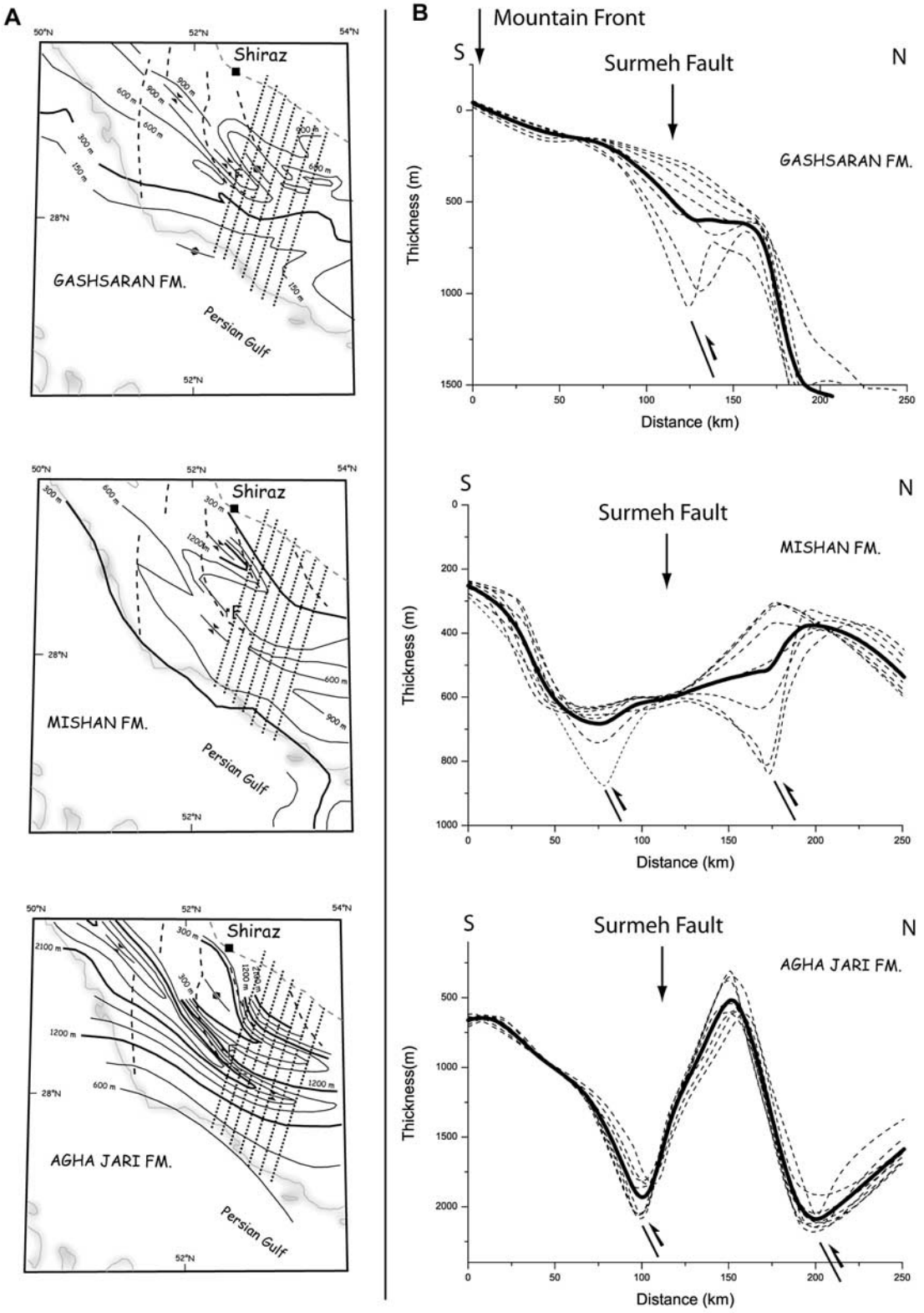

Figure 8. (a) Isopachs of the Gashsaran, Mishan and Agha Jari Formations after a compilation by *Motiei* [1993]. (b) Thickness distribution of formations along eight profiles taken parallel to the transect shown in Figure 8a. The black solid line is calculated by averaging these eight profiles. Half arrows below the profiles aim at locating probable reverse faults that have influenced the position and importance of depocenters in the Zagros foreland basin during the Neogene. F denotes Firuz Abad.

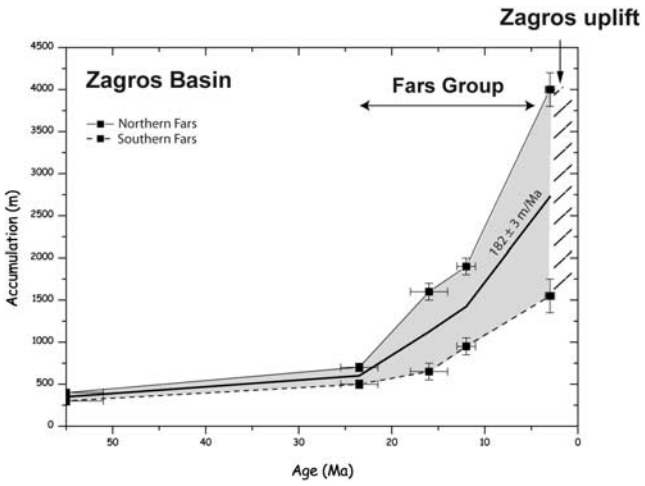

Figure 9. Sediment accumulation over the past 50 Ma estimated from thickness distribution of synorogenic deposits shown in Figure 8. Upper and lower bounds refer to the northern and southern Fars basin, respectively. The black solid line is calculated by averaging both curves. It is clear that sedimentation drastically increase in the Neogene coevally with the collision initiation, shortening, erosion, and uplift in the internal part of the belt (see Figure 19).

These carbonates suggest the preservation of a narrow marine depression in the Central Part of the Zagros basin at this time.

[25] The thickness of the Gashsaran Formation decreases to 150 m close to the Persian Gulf (Figure 8). On the northern limb of the Zalemi anticline, the facies of the Gashsaran Formation is characterized by green-red shales, thin-bedded limestones deposited in intertidal to subtidal environments. At the Mountain Front, on the southern limb of the Asaluyeh anticline, the Gashsaran Formation is locally missing.

[26] The regional across-strike changes in facies reveal the development of a broad coastal plain, including tidal and deltaic deposits to the north, evolving southward to more marine environments. Across-strike thickness distribution further reveals a wedge-shaped subsidence profile typical of foreland basins opens toward the north, i.e., toward the tectonic load. The local abundance of carbonates indicates the presence of a narrow NW–SE-oriented subsident troughs bounded by tidal flats. Northward, it is bounded by a NW–SE-trending paleo-high at the current position of the Surmeh Fault. Variations in the thickness of the Gashsaran/Razak Formations across the Surmeh Fault suggest that deposition was controlled by the fault. The thinning, and locally the lack, of the Gashsaran Formation suggest forebulge-related uplift and/or basement thrusting at the Mountain Front.

4.2. Middle Miocene: Mishan Formation

[27] The Middle Miocene Mishan Formation is characterized by bioclastics and silty carbonates (Figure 10). This sequence may be tentatively correlated with the eustatic rise in sea level reported at the Langhian-Serravalian boundary (~16 Ma) (Figure 6). Close to Firuz Abad, the Mishan Formation consists of mudstones with bivalves and gastropods in association with patched reefal limestones characteristic of infratidal carbonates. The Mishan Formation coarsens upward and passes into bioclastic siltstones and sandstones alternating with shales indicating infratidal to intertidal environment (Figure 10). The thickness of the Mishan Formation increases from 600 m at the latitude of Firuz Abad to about 900 m southward (Figure 8). The thinnest part is found close to the Mountain Front with only 300 m. While the area south of the Karebass-Surmeh Fault is subsident, the northern Central Fars, limited by the Sabz-Pushan and the Karebass strike-slip faults, shows lower accumulation. Hence, by contrast with the Lower Miocene period, the northern Central Fars was uplifted over distance larger than 50 km supporting basement block faulting in the Middle Miocene.

[28] Structural pattern and facies variations in relation with the Meymand and Dalu anticlines deserve further consideration. Their bended axes outline the presence of an underlying active basement feature: the Sabz-Pushan right-lateral strike-slip fault [*Berberian*, 1995; *Lacombe et al.*, 2006]. The Mishan Formation (Guri member) is represented by reefal carbonates, which form linear ridges in the limbs of both folds (Figures 10c, 10d and 10e). Twenty kilometers northward of the Dalu anticline, these ridges disappear and the carbonates are replaced by more siliciclastics and thinner carbonates beds that are not distinguishable from the Razak Formation. It is worth noting that the reefs disappear to the west of the Sim anticline, i.e., exactly above the trace of the NNW–SSE-trending Sabz-Pushan fault zone (Figure 10f). In addition, where Sim and Meymand fold axes connect, the reefal carbonates of the Mishan Formation (Guri Member) lie unconformably above the Gashsaran Formation (Champeh Member) (Figure 10g). We therefore infer that basement-involved deformation associated with transpressive right-lateral strike-slip faulting was active during the Middle Miocene. In summary, the depositional patterns and the facies variations within the Lower and Middle Miocene strata reveal wavelengths and amplitudes of tectonically-induced perturbations that could support basement-involved deformation.

5. Miocene-Pliocene Wedge-Top Basin: Evidence for Inception of Cover Folding

[29] By the end of the Miocene, owing to continuing convergence, contraction resulted in shortening and folding of preorogenic margin sequences and syn-orogenic foreland sequences were deposited in synclinal depressions. The presence of intraformational unconformities within the Agha Jari Formation has been recognized for years in association with thin-skinned folding in the Dezful or Lorestan areas [e.g., *Hessami et al.*, 2001; *Sherkati et al.*, 2005]. However, no evidence for such unconformities has been described in the Central Fars so far. In addition, to our knowledge, no systematic structural study has been carried

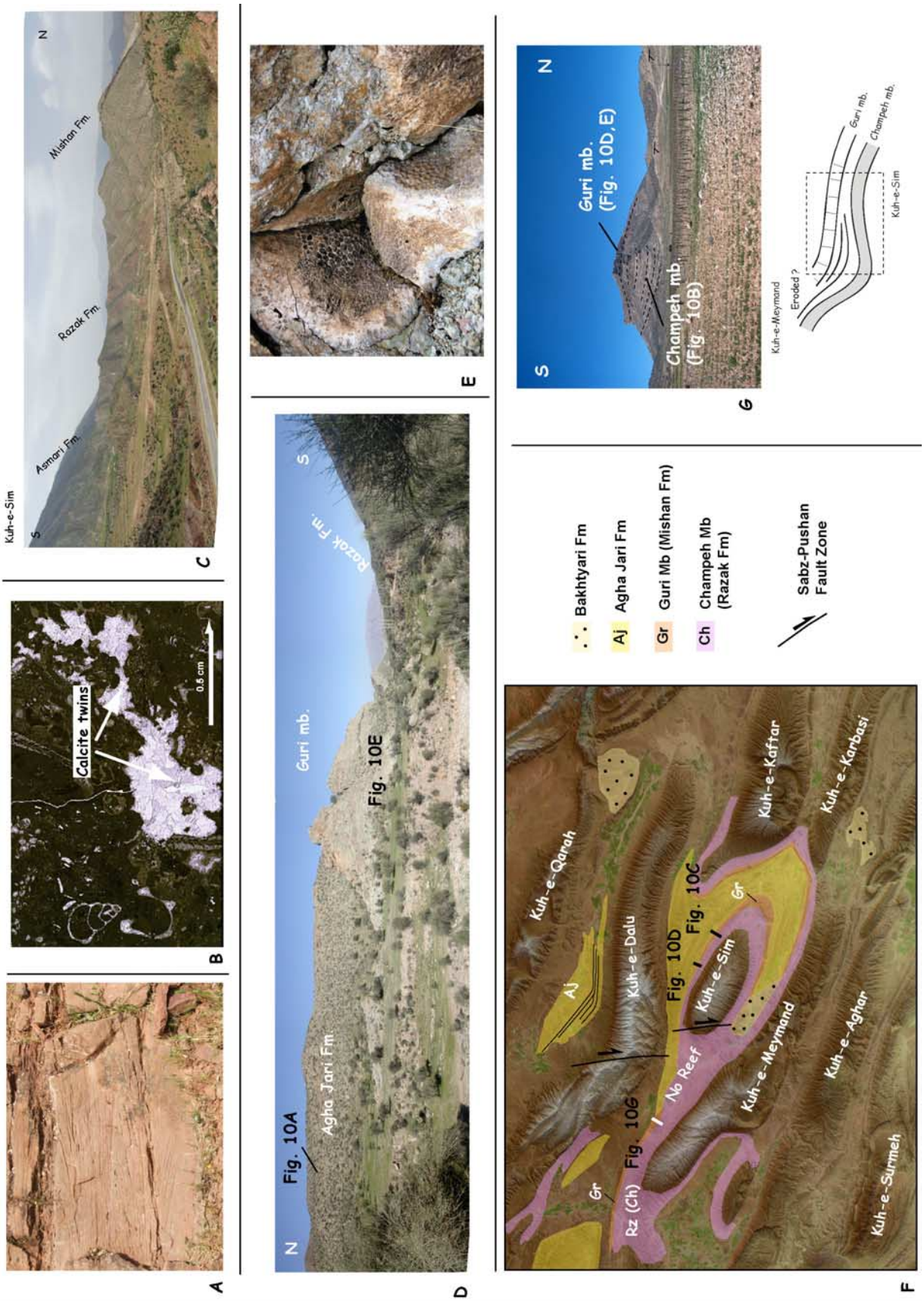
A
B
Calcite twins
0.5 cm
C
Kuh-e-Sim
N
S
Mishan Fm.
Razak Fm.
Asmari Fm.
D
N
S
Fig. 10A
Agha Jari Fm.
Guri mb.
Fig. 10E
Razak Fm.
E
G
N
S
Guri mb.
(Fig. 10D, E)
Champeh mb.
(Fig. 10B)
Kuh-e-Meymand
Eroded ?
Guri mb.
Champeh mb.
Kuh-e-Sim
Bakhtyari Fm
Aj Agha Jari Fm
Gr Guri Mb (Mishan Fm)
Ch Champeh Mb (Razak Fm)
Sabz-Pushan Fault Zone
F
Kuh-e-Qarah
Aj
Kuh-e-Dalu
Fig. 10D
Fig. 10C
Kuh-e-Sim
Gr
Kuh-e-Kaftar
Kuh-e-Karbasi
Rz (Ch)
Fig. 10B
No Reef
Kuh-e-Meymand
Kuh-e-Aghar
Kuh-e-Surmeh

Figure 10

out in the Central Fars to discuss the timing of folding. We aim at filling this gap by examining what are the unconformities that can be observed within the Fars Group and where they are positioned stratigraphically and across the ZFB. To this aim, we have performed numerous field campaigns from Shiraz to the Persian Gulf coast. Owing to the sediment filling, we had usually access to the limbs of anticlines only, lacking data in synclines and making the recognition of synfolding unconformities difficult.

5.1. Molasse Deposits: Agha Jari and Bakhtyari Formations

[30] The Agha Jari Formation usually displays an increasing upward abundance of red weathered shales and sandstones and the complete disappearance of carbonates. Isopachs of Figure 8 show that the Zagros foredeep was more subsident over this period than during the previous ones. The subsidence also increases significantly northward in agreement with the flexure of the Arabian margin undergoing tectonic loading.

[31] A NW–SE-trending high (300 m) and low (2100 m) across the Surmeh Fault suggests that basement-involved thrusting was ongoing in the Zagros foredeep at this time. This is also demonstrated in the bended syncline between the Dalu and Qarah folds. A Landsat image reveals the presence of an unconformity within the Agha Jari Formation (Figure 10f). In the northern limb of the E–W-trending segment of the Dalu anticline, strata of the Agha Jari Formation onlap older strata in a direction oblique to fold axis. Because this angular unconformity is observed close to the trace of the Sabz-Pushan transverse fault we infer it may be related to the presence of a paleo-high in relation with the activity of this strike-slip basement fault at that time.

[32] In summary, the Agha Jari deposits were deposited in a flexural basin within which second-order basement-involved faulting occurred. In the studied area, the facies of the upper Agha Jari Formation laterally change from tidal red silts and shales, dominant to the south, to alluvial conglomerates in the north. In contrast, the Bakhtyari conglomerates, which have been deposited unconformably throughout the ZFB correspond to a period of relative inactivity in the foreland basin. The burial of the folded belt below the Bakhtyari conglomerates is consistent with an overfilled stage. Though the Agha Jari conglomerates can be sometimes mistaken for the Bakhtyari conglomerates in the northern Fars, the mode of deposition of the Bakhtyari conglomerates is different: the Bakhtyari conglomerates blanket and fill a preexisting topography, for example, the synclinal valleys of folds or larger-scale depressions caused by basement-involved deformation. Such a type of deposition allows for the identification of the Bakhtyari Formation as it systematically onlaps toward the folds crest or directly lies unconformably.

5.2. Constraints on the Timing of Folding From Syn-Folding and Post-Folding Unconformities

[33] In the Lorestan province of the Zagros (Figure 1), where magnetostratigraphic constraints exist, the base of the Agha Jari Formation is dated as Serravalian-Tortonian (~12 Ma) [*Homke et al.*, 2004]. The ages of the upper Agha Jari Formation (including the Labhari Member), which is synfolding in the Lorestan, range between 7 and 3 Ma and the overlying conglomeratic layers of the Bathtyari Formation, are younger than 3 Ma. Unfortunately, stratigraphic constraints on the continental molasse deposits are not yet available in our studied area. We have consequently used dating available in the Lorestan area. The maximum age uncertainty is expected in the northern part of the folded belt where continental deposits including Agha Jari and Bakhtyari Formations might be older as they were accumulated for a longer period of time in the more subsident part of the Zagros flexural basin. Taking into account the existing stratigraphic correlations made with reference to biostratigraphic constraints in the underlying carbonates of the Guri member (Figure 6) the continental formations are not older than 10 Ma.

[34] Additional constraints are provided by field observations. The conglomerates, which are synfolding to the North of Shiraz (Figure 11a) are attributed to Plio-Pleistocene Bakhtyari Formation. These deposits are also overlain unconformably by younger conglomerates. If we consider that the Bakhtyari Formation is defined by a post-folding regional unconformity, the oldest conglomerates should belong to the upper Agha Jari Formation. In the absence of other time constraints, these observations provide lower and higher stratigraphic bounds for the synfolding strata of the upper Agha Jari Formation whose age has been set to 5.5 ± 2.5 Ma. The age of the base of the Bakhtyari

Figure 10. Facies and microfacies of the Fars Group in the northern part of the Zagros Folded Belt, in the vicinity of the Sim anticline (see Figure 2 for location). (a) Megaripples in red silts and sandstones of the Agha Jari Formation indicating tidal environment. Note that the older strata of the Razak Formation are very similar in this part of the ZFB. (b) Photograph of a thin section illustrating microfacies of shallow-water bioclastic carbonates belonging to the Champeh Member (Razak-Gashsaran Formation). Calcite twins in vesicles have been used to estimate differential stresses (Figure 4) across the whole ZFB [*Lacombe et al.*, 2007]. (c) Structural relationships between Asmari, Razak and Mishan Formation on the northern of the Sim anticline (no evidence for unconformity has been found). (d) Western boundary of the reefal carbonates of the Guri member on the northern limb of the Sim anticline. (e) Massif corals in the Guri member. (f) Location map of the Sim anticline area near Meymand. (g) Structural relationships between the Guri reefal carbonates and the underlying carbonaceous member (Champeh member) of the Razak-Gashsaran Formation to the west of the Sabz-Pushan Fault Zone. The Guri member lies unconformably above the Champeh member where the Sim anticline connects with the Meymand anticline.

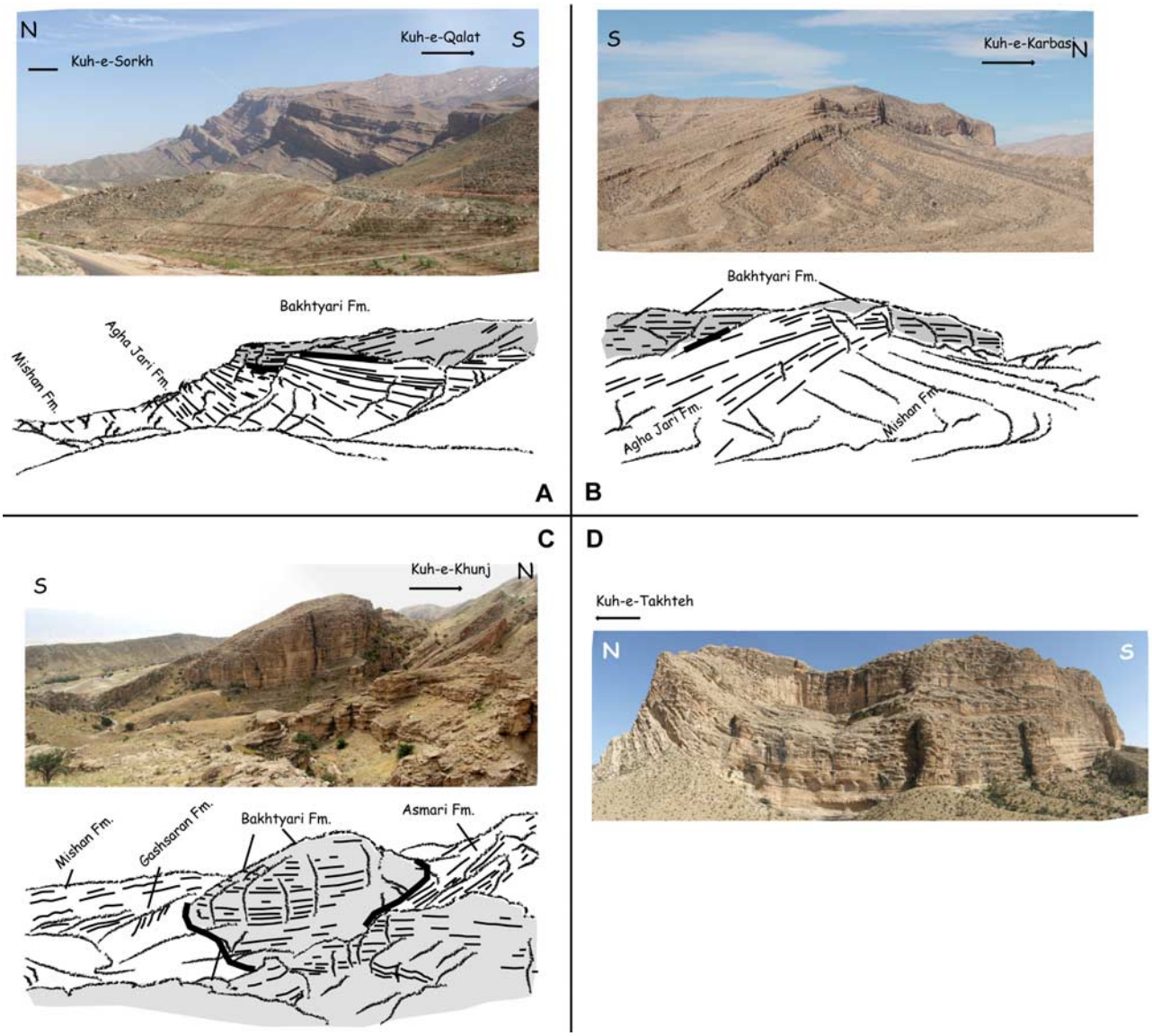

Figure 11. (a) Intraformational unconformities clearly depicted within the upper Agha Jari strata, on the southern limb of the Sorkh anticline (see Figure 2 for location). Above, the conglomeratic beds of the Bakhtyari Formation are onlapping the Agha Jari Formation. This suggests a slowing down of fold growth relatively to sedimentation rates. A subsequent stage of folding in association with the growth of the Qalat anticline is revealed by the tilting of the Bakhtyari conglomerates. (b) Intraformational unconformities within the upper Agha Jari strata on the southern limb of the Karbasi anticline (see Figure 2 for location). The cliff shows the upper alluvial conglomerates of the Bakhtyari Formation. They clearly onlap the older strata of the Agha Jari, again suggesting a slowing down of fold uplift. (c) Bakhtyari conglomerates overlying unconformably older strata of the Fars Group and carbonates of the Asmari Formation on the southern limb of the Khunj anticline indicating significant erosion prior to the deposition of the conglomerates. (d) Folded Bakhtyari conglomerates on the southern limb of the Takhteh anticline.

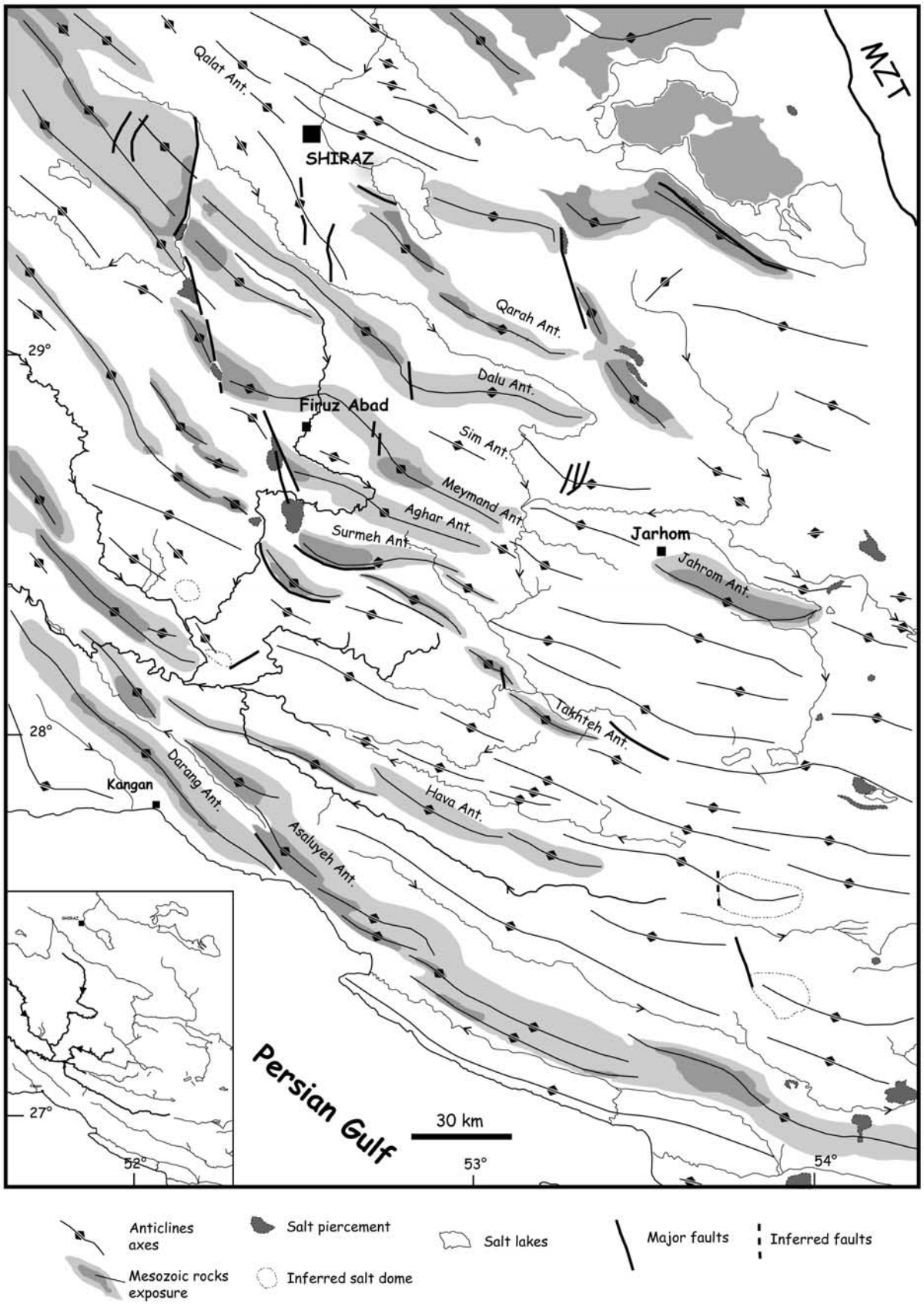
MZT
SHIRAZ
Qalat Ant.
Qarah Ant.
Dalu Ant.
Firuz Abad
Sim Ant.
Meymand Ant.
Aghar Ant.
Surmeh Ant.
Jarhom
Jahrom Ant.
Takhteh Ant.
Darang Ant.
Kangan
Hava Ant.
Asaluyeh Ant.
Persian Gulf
30 km
29°
28°
27°
52°
53°
54°
Anticlines axes
Salt piercement
Salt lakes
Major faults
Inferred faults
Mesozoic rocks exposure
Inferred salt dome

Figure 12

Formation is considered to be 3 ± 0.5 Ma throughout the belt. The age of the top of the Bakhatyari conglomerates has been roughly approximated by taking advantage of the relation between thickness and the extrapolation of maximum sedimentation rates (Figure 9). The absolute ages presented in the following sections should be considered as indicative estimates for forthcoming studies on fold kinematics.

5.2.1. Sorkh and Qalat Anticlines: Northern Fars

[35] Twenty kilometers to the North of Shiraz and just south of the High Zagros Fault (Figures 3 and 11a), above marls, sands and carbonates of the Mishan Formation, conglomerates attributed to the Upper Agha Jari show progressive unconformities revealing syn-sedimentary rotation on the southern limb of the Sorkh anticline. The upper part of the outcrop shows conglomerates that are dipping toward the north on the northern limb of the Qalat anticline. These latter are consequently onlapping older conglomerates and would better correspond to the younger Bakhtyari Formation. We deduce that the last increment of deformation of the Qalat anticline mainly postdates the development of the Sorkh anticline, which initially grew by limb rotation during the deposition of the upper Agha Jari conglomerates at 5.5 ± 2.5 Ma. This episode is followed by a decrease in the fold uplift rate relative to the rate of accumulation of upper Bakhtyari conglomerates. To figure out the age of the Qalat fold we extrapolate the thickness of strata to the average sedimentation rates (Figure 8). Taking into account that at least 100–200 m were deposited, we obtain a maximum age of 2.5 − 2 ± 0.5 Ma for the top of the conglomerates and hence for the last folding event.

5.2.2. Karbasi Anticline: Central Fars

[36] Progressive unconformities are also found in the southern limb of the Karbasi anticline about 200 km southeastward of the Sorkh anticline (Figures 3 and 11b). The progressive unconformities are found in the lower and older strata belonging to the upper Agha Jari Formation. The cliff formed by the Bakhtyari conglomerates again displays no evidence for intraformational unconformity. We thus conclude to a similar Pliocene sequence of folding as for the Sorkh anticline. After Karbasi anticline developed by limb rotation 5.5 ± 2.5 Ma ago, the Bakhtyari conglomerates were deposited unconformably during a period of relative folding quiescence.

5.2.3. Khunj Anticline: Southern Fars

[37] The Khunj anticline, in the Central Fars, is located in an elongated faulted belt aligned along the Surmeh fault (Figures 3 and 11c). According to existing geological maps and satellite images its southern limb is suspected to be faulted. However, we observe a remnant patch of Bakhtyari conglomerates that overlie unconformably the folded strata of the Gashsaran and Asmari formations. Although no structural relationship has been found between the Agha Jari Formation and the Bakhtyari conglomerates, we suspect that the latter lie unconformably above the Agha Jari Formation. The Bakhtyari conglomerates are made of pebbles of carbonates, which are essentially flat. In contrast with the Qalat anticline, but similarly with the Karbasi anticline, the main phase of folding seems to have ceased before the deposition of the Bakhtyari Formation at 2.5 − 2 ± 0.5 Ma.

6. Constraints on Quaternary Fold Growth and Its Relationships With Active Basement Faulting: Insights From Morphology, Drainage Pattern, and Historical Seismicity

6.1. Regional Versus Local Drainage Pattern: The Role of Thick-Skinned Deformation

[38] Studies dealing with morphological patterns in the Zagros Folded Belt date back to tens of years with reference to the drainage pattern observed in the Dezful area [*Oberlander*, 1985; *Tucker and Slingerland*, 1996]. The main transverse streams observed in the Zagros Folded Belt form spectacular river gorges in the Dezful area [*Oberlander*, 1985]. Then they join the Tigris-Euphrates rivers or flow directly into the Persian Gulf. Remarkably, the Central Fars is characterized by a lack of evidence for river antecedence (or superposition) and N–S transverse drainage throughout the folded belt (Figure 12). Rivers do not follow a simple south-flowing course across the folded belt and have a course shorter than axial rivers. This drainage pattern suggests that rivers are strongly controlled by the folds growth. Deviation of the course of rivers may be explained as the result of transverse rivers being dammed by the uplift of major anticlines.

[39] It should be noted that the sinusoidal shape of folds is superimposed on background uplift controlled by basement involvement that is outlined by a regional topography sloping at 0.3°–0.5° toward the foreland [*Mouthereau et al.*, 2006]. The drainage network is thus expected to be controlled to some extent by thick-skinned deformation. For instance, north of the Karebass-Surmeh faults segment, most rivers are forced to flow axially toward the east. This is the response of the tilting of the regional base level toward the east caused by the deformation associated with a set of oblique transpressive ridges: the Surmeh-Karebass and the Sabz-Pushan faults segments (Figure 12).

[40] In the center of the Fars arc, east of longitude 53.5°E, we identify a domain where the drainage patterns do not show any preferential flowing orientation and where most of the northern transverse rivers rapidly die out in several salt depressions. This endoreic fluvial system is disconnected from the main western fluvial system debouching in the Persian Gulf. Such intermontane depressions, which are associated with a decrease of channel gradient, reopens

Figure 12. River drainage network in the Zagros Folded Belt reconstructed on the basis of Landsat images. Inset in the lower left show drainage network in the absence of structural information. The rivers flowing toward the south are closely related with largest slope gradient near active basement-involved fault zones. Away from these domains, rivers often flow axially or die out into the Central Fars depression.

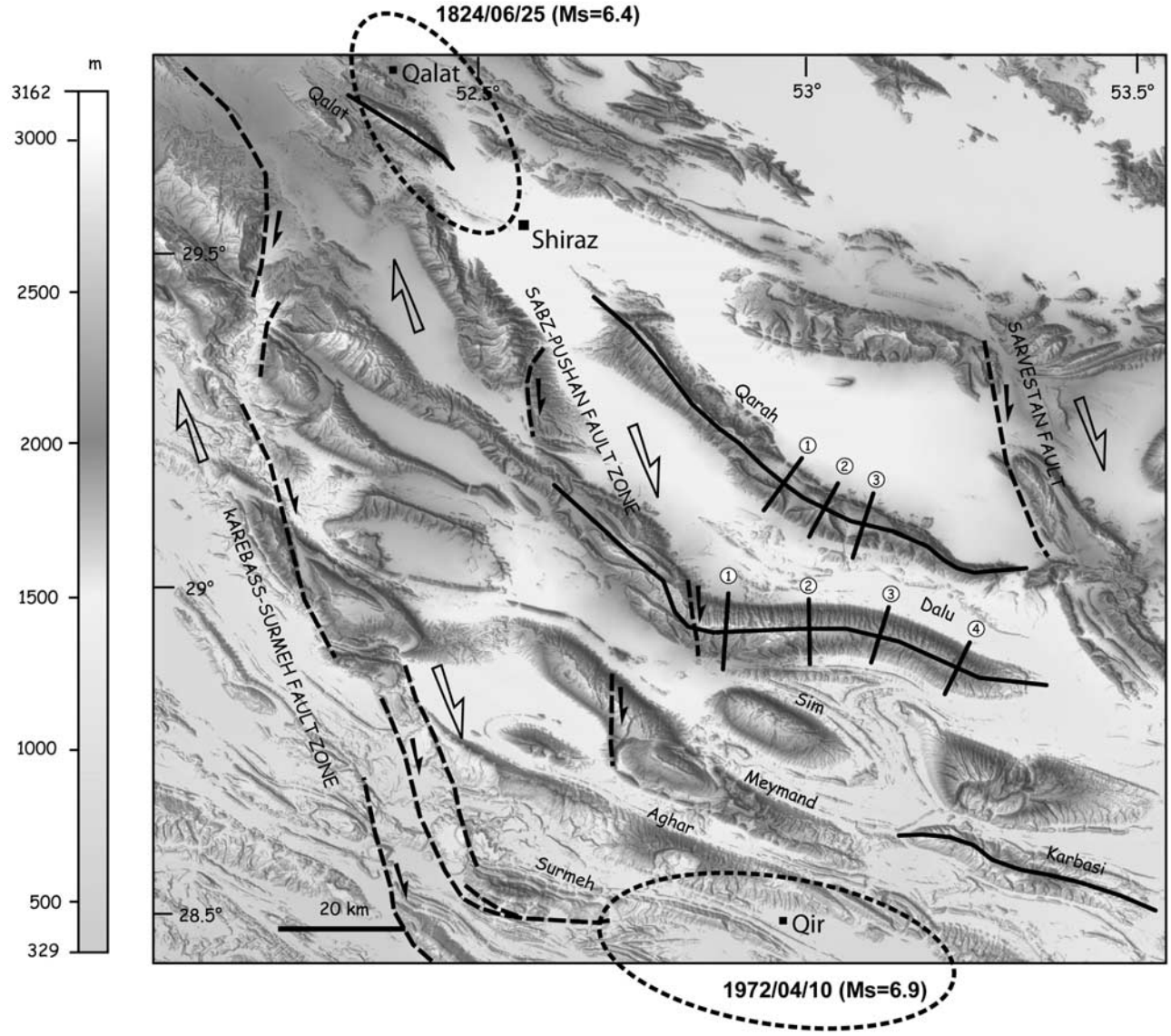

Figure 13. Digital elevation model of the Fars Province (northern domain) based on SRTM data with 90 × 90 m resolution. Anticlines mentioned in this study are shown together with the location of axial and transverse topographic profiles. Major strike-slip fault zones that affect the sedimentary cover are also depicted. Black dashed ellipsoids correspond to the areas destroyed during major earthquakes of years 1824 near Qalat and 1972 (Qir earthquake) after *Ambraseys and Melville* [1982].

progressively to the south as the slope, increasing in the footwall of the active Surmeh fault, allows rivers to flow again transversally. Again southward, the rivers flow axially to the West, and merge before debouching in the Persian Gulf, north of the Mountain Front Fault.

[41] As already inferred from observations of isopachs (Figure 8), we propose Quaternary basement-involved shortening produced topographic highs and lows that controlled the regional course of rivers. Growing folds likely secondarily created abnormal southeast or southwest flowing streams by forcing rivers to flow axially. This is particularly clear in the vicinity of the Dalu anticline to the northern Central Fars and the fold system of Hava, Zalemi or Asaluyeh anticline closer to the Mountain Front (Figure 12).

6.2. Fold Uplift and Basement Faulting: Geomorphic and Seismotectonic Constraints

[42] The degree of removal of weakly cemented and siliciclastics strata of the Fars group above the competent beds of the Asmari Formation may serve as a proxy for relative age of folds. To a first approximation, assuming initially constant cover thickness, fold growth rates and river stream power, the oldest anticlines would be those where Mesozoic rocks crop out owing to more bedrock uplift or incision (Figure 13). However, several other

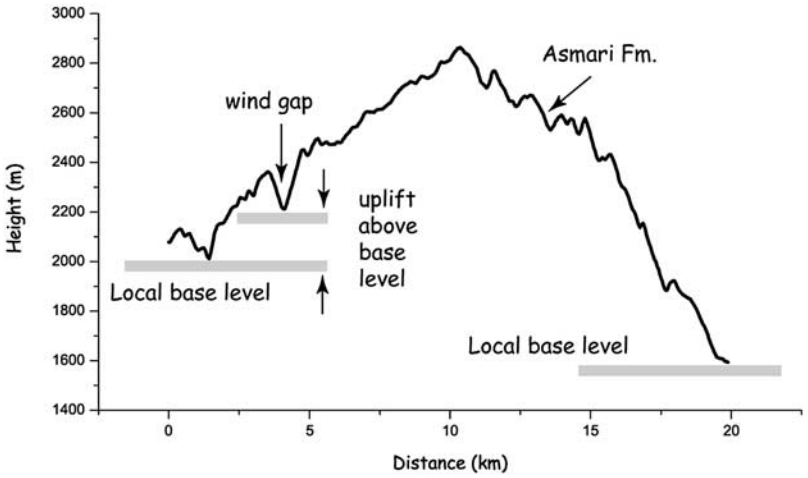

Figure 14. Axial topographic profile across the Qalat anticline. See Figure 13 for location.

parameters may additionally control the geomorphic signature of folds in foreland such as (1) the ratio of the sediment accumulation to the structural uplift, (2) the balance of the stream power versus the bedrock resistance and the rates of fold uplift [*Burbank et al.*, 1996; *Tucker and Slingerland*, 1996] or (3) the initial thickness of weakly cemented rocks.

[43] We have noticed that one remarkable feature of the Central Fars is the lack of rivers cutting through the anticlines, with noticeable exceptions in areas where basement uplifts have been recognized. This would imply that the structural uplift was too rapid for rivers to cut down through the fold. Moreover, a simple in-sequence cover folding development in the cover is unlikely in the Central Fars as it would have certainly resulted in antecedence or superposition of rivers through the folded belt as exemplified in the Apennines [*Alvarez*, 1999]. This would further imply that all folds possibly formed nearly at the same time. Hereafter, we focus on this latter possibility and the possible control by inherited fault-controlled basement highs.

6.2.1. Qalat Anticline

[44] The Qalat anticline is one of the few folds for which a significant part of contraction seems to postdate the deposition of the Bakhtyari conglomerates. It developed in the southern limb of the Sorkh fold revealing, at least locally, a southward in-sequence propagation of folding. The fold wavelength, defined by the distance between two adjacent synclinal axes, is 13 km consistent with the typical fold wavelengths in the Central Fars (Figure 5). A NW–SE axial topographic profile shows that the minimum total uplift of the Asmari surface is 1300 m relative to the eastern local base level. Along the axial profile we also notice a differential topographic elevation of local base levels: the eastern nose of the fold is 400 m lower than the western one (Figure 14) and the latter shows a wind gap within the Asmari carbonates. This illustrates the ongoing westward propagation of folding. Since the abandonment of the river, the fold was uplifted by about 200 m.

[45] Given a minimum structural uplift of the Asmari surface of 1300 m relatively to the eastern local base level and an age of $2.5 - 2 \pm 0.5$ Ma for the inception of fold uplift, we deduce that fold uplifted at a rate of 0.58 ± 0.22 mm/yr. In addition to thin-skinned folding, we challenge that the morphology of the Qalat anticline might have been also influenced by basement-involved deformation. Indeed, a destructive earthquake ($M_s = 6.4$) that occurred in 1824 (25 June) damaged the city of Shiraz and the city of Qalat was ruined and a few hundred people were killed [*Ambraseys and Melville*, 1982]. *Berberian* [1995] noted that the destruction area related to the earthquake is elongated NNW–SSE, parallel to the northern extension of the Sabz-Pushan transverse fault. We infer that the current morphology of the Qalat anticline might be largely related to vertical movements along the right-lateral Sabz-Pushan fault zone.

6.2.2. Qarah and Dalu Anticlines

[46] The Qarah and Dalu anticlines are subparallel and distant by 15–25 km (Figures 10 and 13). The axial topographic profile across the Qarah anticline shows important denudation in the center of the anticline. Its wavelength is abnormally larger than 20 km. A comparison of the transverse topographic profiles 1, 2, 3 with the axial profile provides an estimate for the volume of pre-Asmari rocks removed by erosion, which is of the order of 60 km^3 (Figure 15). The Mesozoic strata are exposed within the anticline in two large wind gaps, which are weakly elevated in regard to adjacent base levels. This would suggest the absence of recent fold uplift. The Dalu fold, to the south, is a drag fold that developed above the active Sabz-Pushan right-lateral strike-slip fault zone (Figures 10 and 13). By contrast with the Qarah anticline, the Dalu anticline shows much less denudation as illustrated by the slightly dissected structural surface of the Asmari carbonates (Figure 15). Its fold wavelength of 12–15 km is also shorter and the minimum uplift of the Asmari surface with respect to the local base level is larger, i.e., ~1800 m on average. The presence of a water gap in the eastern nose of the fold suggests that eastward propagation of the fold is still ongoing, away from the Sabz-Pushan fault zone. These

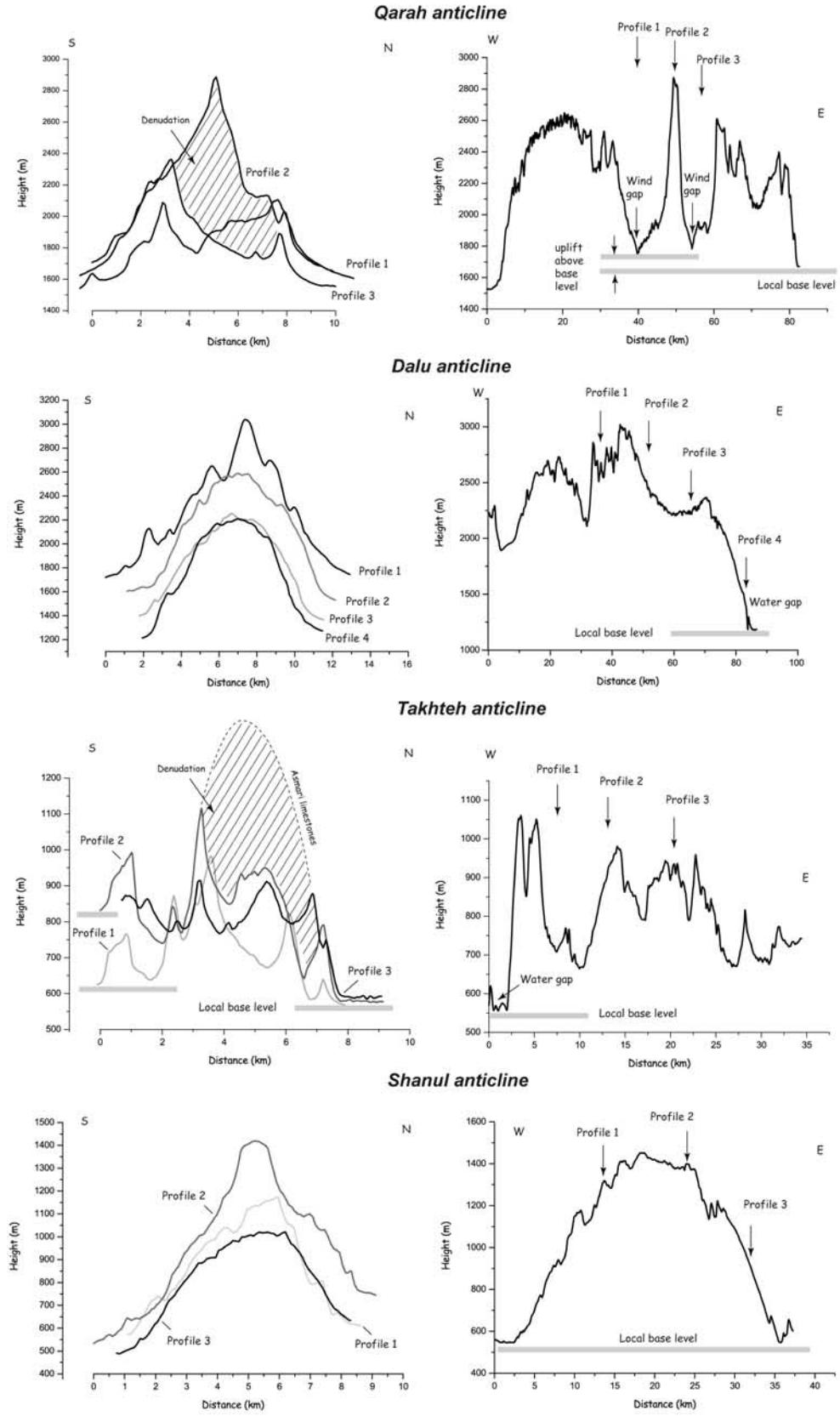

Figure 15. (left) Transverse and (right) axial topographic profiles of the Qarah, Dalu, Takhteh, and Shanul folds. See location in Figures 13 and 16.

geomorphic data may suggest that the Dalu fold may be younger than the Qarah fold.

[47] In 1892, a macroseismic earthquake have been reported exactly in this bended portion of the Dalu anticline [*Berberian*, 1995], which confirms the still ongoing deformation along the Sabz-Pushan basement fault. Because isopach maps and field observations both indicate that this area was controlled by the activity of the Sabz-Pushan fault zone as soon as the Middle-Upper Miocene times, we suggest that the sequence of thin-skinned folding between Qarah and Dalu anticline was also influenced by thick-skinned deformation along the NNW–SSE-trending transpressive ridge of the Sabz-Pushan Fault Zone. This may explain (1) the abandonment of transverse rivers cutting through the Qarah anticline and (2) to some extent, the origin of the Dalu anticline itself.

6.2.3. Takhteh Anticline

[48] The Takhteh anticline lies within a girdle of en-échelon folds aligned along the trend of the active Surmeh fault (Figures 11d, 14, and 15). It is characterized by a fold wavelength of 13–14 km and the presence of folded Bakhtyari conglomerates. The current activity of the Surmeh fault is revealed by the 1972 Qir earthquake (M_s = 6.9), which killed about 5000 people [*Ambraseys and Melville*, 1982]. Similarly with the Qarah anticline, the Mesozoic cover is well exposed within the Takhteh anticline indicating that the fold was deeply eroded. Differential N–S elevation across the fold (Figure 15) is explained by the axial west-flowing river, which has wiped out the Bakhtyari conglomerates deposited in the northern fold limb. This contrasts with the southern limb where the Bakhtyari conglomerates are thick and form cliffs (Figures 11d and 15). A significant part of the shortening postdates the deposition of the Bakhtyari conglomerates such as for the Qalat fold (Figure 11d). To explain the apparent inconsistency between the smooth fold morphology and the fact that Bakhtyari Formation is folded, it is important to consider that the Takhteh anticline developed in the vicinity of a Miocene paleo-ridge (Figure 8). The Cenozoic strata were initially thinner than in adjacent areas so it may have been more rapidly incised by rivers. On the basis of extrapolation of sedimentation rates, and taking into account that the pre-folding Bakhtyari conglomerates are not thicker than 200 m, we deduce that the top of the conglomerates should be $\sim$2 ± 0.5 Ma. Given a minimum total uplift of 700 m, we infer a maximum uplift rate of 0.33 ± 0.25 mm/yr.

6.2.4. Shanul Anticline

[49] The Shanul anticline is located 40 km to the south of the Takhteh anticline (Figures 15 and 16). It has a wavelength of 13–14 km comparable with Qalat, Dalu and Takhteh folds. A major difference however is that its structural topography is outlined by the resistant carbonates of the Mishan Formation. Transverse and axial topographic profiles show that the Mishan Formation is not significantly eroded (Figure 15). Given the altitude of the Mishan carbonates, the fold uplift with respect to the adjacent local base levels is about 900 m. To explain this particular morphologic pattern we must again refer to the isopach maps (Figure 8). They show that this area was a main Mishan depocenter in the footwall of the Surmeh Fault. As the rivers incised a thicker Neogene sequence, only a limited part of the upper layers overlying the competent Mishan carbonates were removed. This is consistent with the fact that in contrast with folds located in the hangingwall of the Surmeh Fault, the local base levels at both noses of the fold reveal little incision by rivers and even deposition in the large synclinal valleys. We suggest that the age of folding may not be significantly different from that of Qalat, Dalu and Takhteh anticlines.

6.2.5. Mountain Front

[50] The deformation at the Mountain Front close to the Persian Gulf is characterized by a 200-km-long girdle of five en-echelon anticlines in the hangingwall of the Mountain Front Fault (Figure 16). The current activity of this major basement reverse fault is revealed by the series of recent historical and instrumental earthquakes: two macroseismic earthquakes have been reported in 1883 (M_s = 5.8) whose destruction area is aligned in the direction of the Asaluyeh anticline (Profile 1) and more recently in 1950 (M_s = 5.5) [*Ambraseys and Melville*, 1982; *Berberian*, 1995].

[51] The anticlines have wavelengths of about 20 km, on average, larger than Qalat, Dalu, Takhteh and Shanul anticlines but close to the wavelength of the Qarah anticline. The maximum total uplift of the folds with respect to the Persian Gulf increases from 800 m (profile 5) and 1400 m (profile 1) northwestward (Figure 17). The remarkable differential elevation of 200 to 700 m of local base levels across the Mountain Front folds is controlled to first-order by basement thrusting along the Mountain Front Fault. Furthermore, local tilting of Quaternary terraces near the Mountain Front [e.g., *Mann and Vita-Finzi*, 1988], geodetic surveys [*Walpersdorf et al.*, 2006] as well as ^{14}C dating of Holocene fluvio-marine terraces [*Oveisi et al.*, 2007] shows that a significant part of the deformation in the Zagros is currently accommodated across the Mountain Front.

7. Discussion

7.1. Thin-Skinned Buckling of the Sedimentary Cover

[52] The present study has emphasized particular features of folding: (1) the existence of characteristic fold wavelengths, (2) no thrust is associated with folding at the surface, (3) across the 200-km-width ZFB, folding developed rather synchronously over the past 5.5 ± 2.5 Ma, and (4) the progressive onlaps of conglomerates onto older growth strata (Figure 11) suggest a slowing down of fold growth relatively to the rate of deposition. To explain such results and observations we challenge that the development of the Zagros fold train is better reproduced by invoking buckling of the cover, while both distributed and localized thrusting occurred within the basement.

[53] The theory of buckling predicts that a single competent layer with random perturbations overlying a weaker matrix will develop into a regular fold train when subjected to layer-parallel shortening [*Biot*, 1961; *Zhang et al.*, 1996]. Fold train results from the process of selection and amplification of initial perturbations that is dependent on the

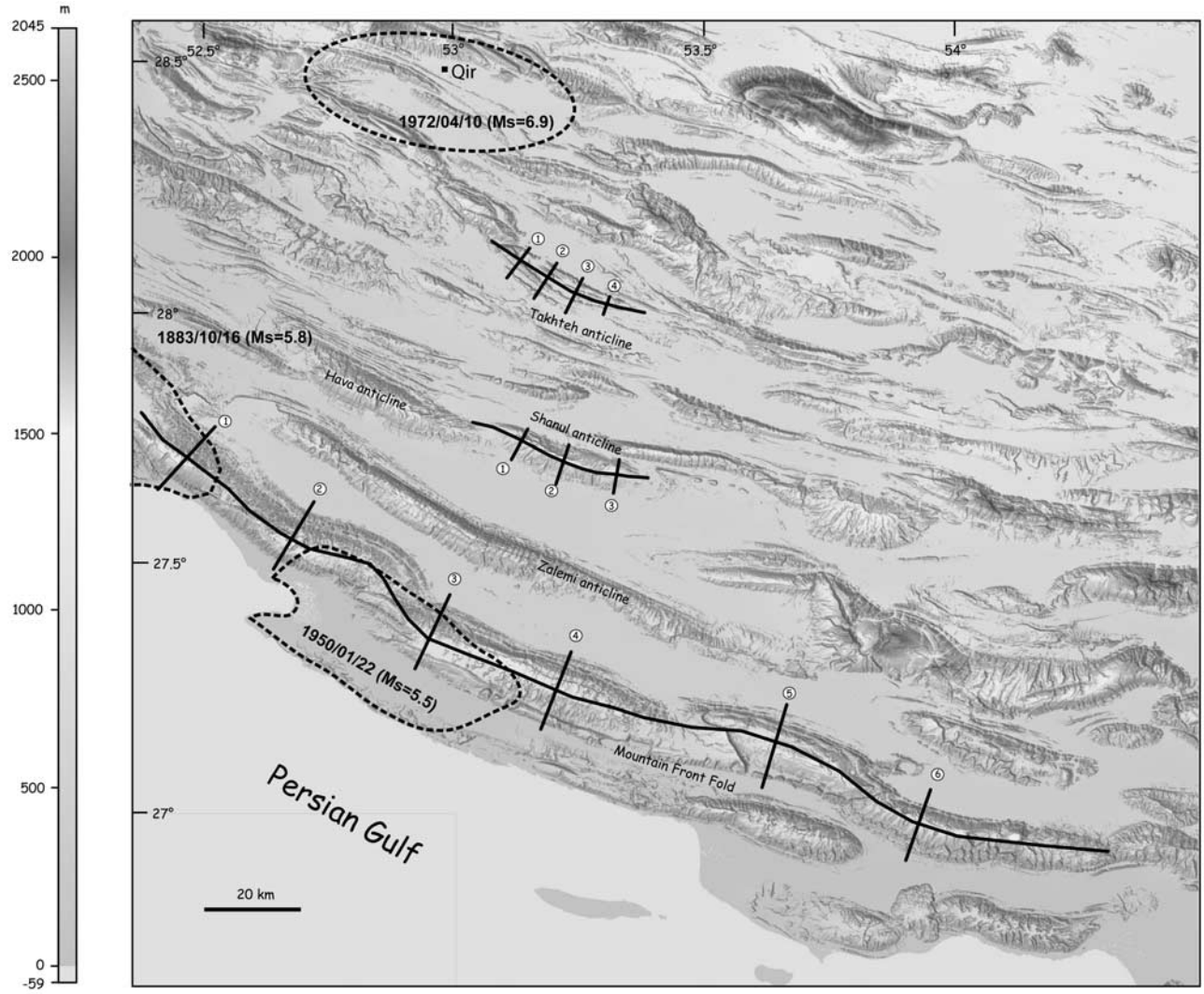

Figure 16. Digital elevation model of the Fars Province (southern domain) based on SRTM data with 90 × 90 m resolution. Anticlines mentioned in this study are shown together with the location of axial and transverse topographic profiles (Figure 15). Black dashed ellipsoids correspond to the areas destroyed during major seismic events that occurred in 1972 (Qir earthquake) and 1950 after *Ambraseys and Melville* [1982].

competency contrasts between matrix and layer. The initiation of fold growth is exponential when the dominant wavelength is selected and then gradually slows down.

[54] Several analytical and numerical models have considered folding in the Zagros fold belt as a case example for studying mechanisms of buckling [*Biot*, 1961; *Schmalholz et al.*, 2002; *Turcotte and Schubert*, 2002]. The thick Paleozoic and Mesozoic carbonates can be treated as a single layer overlying a homogeneous and finite viscous matrix lying in the Cambrian salts. It has been noticed for years that the pure elastic solution for buckling wavelengths given by $2\pi H\sqrt{E/\sigma}$ often requires unrealistic high layer-parallel stress σ to fit observed buckling wavelengths. However, folding wavelengths may be roughly approximated by a pure elastic solution [*Mouthereau et al.*, 2006] assuming a layer-parallel stress σ of at least 300 MPa and a low value of Young's modulus E of 10^9 Pa supported by recent mechanical experiments on Asmari carbonates [*Amrouch et al.*, 2005]. The result is however largely dependent on the effective elastic thickness H adopted for the competent layer. A value of less than 2 km, i.e., representing only a quarter of the value of the unbended layer, is compatible with fold curvatures ($>10^{-5}$ m^{-1}) and brittle yielding in a plastic(brittle)/elastic layer. On the other hand, a pure viscous solution for buckling wavelengths given by $2\pi H 6^{-1/3}\sqrt[3]{\eta_l/\eta_m}$ is limited by viscosity contrasts between layer and matrix of less than 2 orders of magnitudes [*Schmalholz et al.*, 2002]. The viscosity of the Hormuz evaporites has been fixed to typical viscosities (Newtonian) of salts between 10^{17} and 10^{18} Pa s [*Mouthereau et al.*, 2006]. In this case, fold wavelengths may be reproduced using a thin viscous layer H of 2 km and

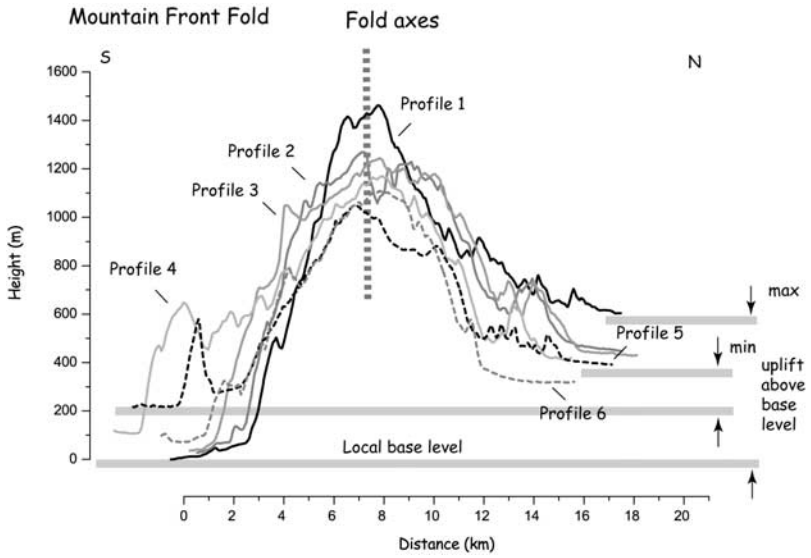

Figure 17. Transverse topographic profiles across-folds associated with the Mountain Front. See location in Figure 16.

layer viscosity η_l of 10^{19} Pa s. We see that none of these end-member models are satisfactory since they consider that only a thin portion of the total thickness of the sedimentary cover is competent. A viscoelastic solution, which consists of an elastic sublayer at shallow depths overlying a viscous (non-Newtonian) sublayer with finite thickness to greater depths seems to reproduce better fold wavelengths [*Schmalholz et al.*, 2002].

[55] In details, the wavelengths of folds are not perfectly homogenous. On the basis of cross section (Figure 4), wavelengths vary from 11 km in the vicinity of the Surmeh fault to a maximum of 30 km in the High Zagros. To the south, toward the MFF, fold wavelengths reduces again to 17 km on average. It is not surprising that the observed wavelengths may be lower than those predicted by models of buckling. After inception of buckle folding and selection of a dominant wavelength, shortening increases thus reducing the wavelengths with time as fold amplitudes increase. We infer that folding initially developed with higher wavelength/amplitude ratio across the ZFB. Then as shortening increased and wavelengths reduced, limbs rotated and amplitudes increased. For instance, the ratios of the wavelength to folds amplitude range from 15 (30:2) in the IZ whereas it decreases to 5.5 (11:2) when approaching the Surmeh Fault (Figure 4). In the IZ, the folds have preserved their initial geometry whereas in the ZFB more shortening led to reduce the wavelengths.

[56] Even though the kinematics of folding cannot be accurately and continuously tracked over time owing to the lack of sufficiently accurate stratigraphic data, there are enough constraints for deciphering the initiation of folding associated with syn-folding sedimentation and limb rotation at 5.5 Ma as well as the subsequent growth stage of folding. One can draw the following scenario (Figure 18). In the Upper Miocene–Early Pliocene, after 5.5 ± 2.5 Ma, folds initially developed rapidly as buckle instabilities with wavelengths larger than 25 km and negligible amplitudes (Figure 18a). As shortening increased, fold wavelengths progressively reduced. Folds grew by limb rotation in association with intraformational unconformities within the upper Agha Jari Formation (Figure 18b). This stage is similar to typical detachment folding and models of folding with constant limb length [*Storti and McClay*, 1995; *Ford et al.*, 1996]. As fold uplift rate decreased relatively to the rate of sedimentation, Bakhtyari conglomerates were deposited unconformably (Qalat, Karbasi, Khunj anticlines) (Figure 18b). By 3 Ma, some folds (Qalat, Dalu, Takhteh, Shanul, Mountain Front) rejuvenated with fold uplift rates of the order of 0.3–0.6 mm/yr. (Figure 18c) This last event is observed in portions of the ZFB where underlying basement deformation occurred and is still ongoing and may thus explain, at least partially, folding. Alternatively, the erosion on the crest of anticlines driven by climatic forcing in the past 3 Ma may have also enhanced folding.

7.2. Sequence of Thin/Thick-Skinned Deformation in the Zagros: From Paleocene Foreland Deposition to Cover Buckling at the Arabia/Eurasia Plate Boundary

[57] Recent studies have pointed out that the outward propagation of the ZFB may have occurred either in a single thin-skinned mode or in a two-step evolution involving a period of thin-skinned deformation followed by a period of thick-skinned deformation. The present study suggests that the sequence of deformation in the whole crust was probably more complex.

[58] The first model was proposed by *Hessami et al.* [2001] who suggested, on the basis of the interpretation of local angular unconformities, that folding in the Central Fars started at the end of the Eocene and then propagated with typical thin-skinned forward-propagating sequence

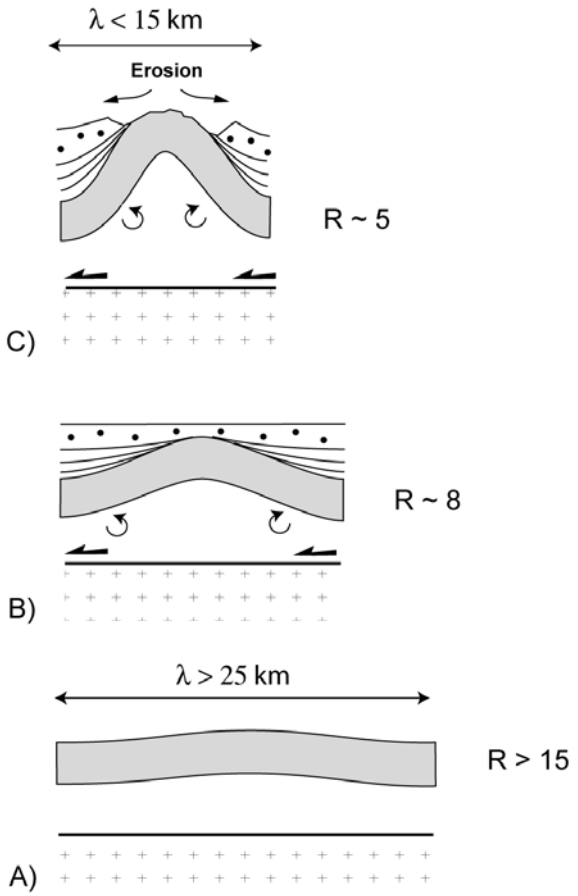

Figure 18. Schematic model of fold development from (a) buckling stage to (b, c) detachment folding involving limb rotation. The gray layer is a schematic representation of the competent (viscous-elastic-plastic) folded cover rocks. The Agha Jari and Bakhtyari Formations are shown as thin white layers overlain by a thick layer with black dots, respectively. R is the ratio of the wavelength to folds amplitude, and λ is the wavelength of folds.

southward. Then *Molinaro et al.* [2005] suggested that the ZFB resulted from two distinct periods: the first being characterized by in-sequence thin-skinned mode since the Middle-Late Miocene and the second by out-of-sequence thick-skinned thrusting since the Pliocene. However, one can draw several limitations to both interpretations. First, the occurrence of in-sequence propagation is not so common in folded belts controlled by a ductile décollement as they often shows rearward propagation [*Costa and Vendeville*, 2002], oscillating sequence of deformation [*Smit et al.*, 2003] or very fast propagation of the wedge front [*Bahroudi and Koyi*, 2003]. Second, none of the available studies satisfactorily account for the coeval involvement of cover (thin-skinned) folding and basement (thick-skinned) deformation currently observed.

7.2.1. From Obduction to Collision

[59] In Figure 19, we synthesize the sequence of deformation from the obduction to the inception of the Zagros collision. The sub-marine obduction of the ophiolites initiated in the Turonian [*Ziegler*, 2001] and lasted until the upper Cretaceous (Campanian). Since then, a narrow trough, filled with up to 1–2 km of hemipelagic carbonates and siltstones of the Gurpi Formation (Maastrichtian), developed to the south of the present position of the MZT [*Koop and Stoneley*, 1982]. This basin reveals the inception of flexural subsidence resulted from the subaerial and ongoing outward advancement of ophiolitic thrust nappes onto the Arabian continental margin. Following this episode, from the Upper Cretaceous—Paleocene and until the Eocene, the environments of deposition significantly changed and the subsidence increased [*Koop and Stoneley*, 1982]. The deposition of 1-km-thick siliciclastic turbidites (Amiran Formation) in the Lorestan province suggests ongoing propagation of the ophiolitic nappes southward [*Homke et al.*, 2007]. Onto the Fars promontory, the turbiditic sequences pass laterally into continental weathered shales or shallow-marine clastics of the Pabdeh-Sachun formations. This region represents the distal, nearly undeflected, portion of the foreland basin. Foreland deposits are overlain by Eocene reefs and dolomites of the Jahrom Formation in the Fars platform passing to Eocene turbiditic sequences as reported on top of the obducted units northward [*Hempton*, 1987; *Beydoun et al.*, 1992] suggesting a flexurally controlled subsidence.

7.2.2. Inception of Collision and Development of the Thin-Skinned/Thick-Skinned Collision Belt

[60] The early Neogene period is characterized by the deposition of carbonates throughout the Arabian continental margin (Asmari Formation) and the Iranian plateau (Qom Formation). These are intertidal boundstones, micritic and foraminiferal limestones, including mainly nummulites and miliolids within the Asmari Formation. Biostratigraphic constraints yield ages ranging from Upper Oligocene to Lower Miocene for both formations (Chattian-Aquitanian boundary) [*Schuster and Wielandt*, 1999]. The Iranian Plateau and the Zagros Folded Belt, which were below sea level at that time, are separated from each other by a NW-

Figure 19. Reconstruction of the Zagros evolution from obduction to collision. Mesozoic strata, are given in green color, Paleogene in orange and the Neogene in yellow (see inset captions for details). White arrows pointing upward indicate uplift whereas black arrows pointing downward are for subsidence. Erosion and orientation of sediment supply from uplifted areas is indicated by smaller black arrows. ZFB, Zagros Folded Belt; IZ, Imbricate Zone. Note that since 3–2 Ma the Imbricate Zone and the MZT are inactive. The current seismogenic deformation has been transferred southward toward the Mountain Front, which attests for southward propagation of the basement wedge and part of the convergence accommodation across the Mountain Front.

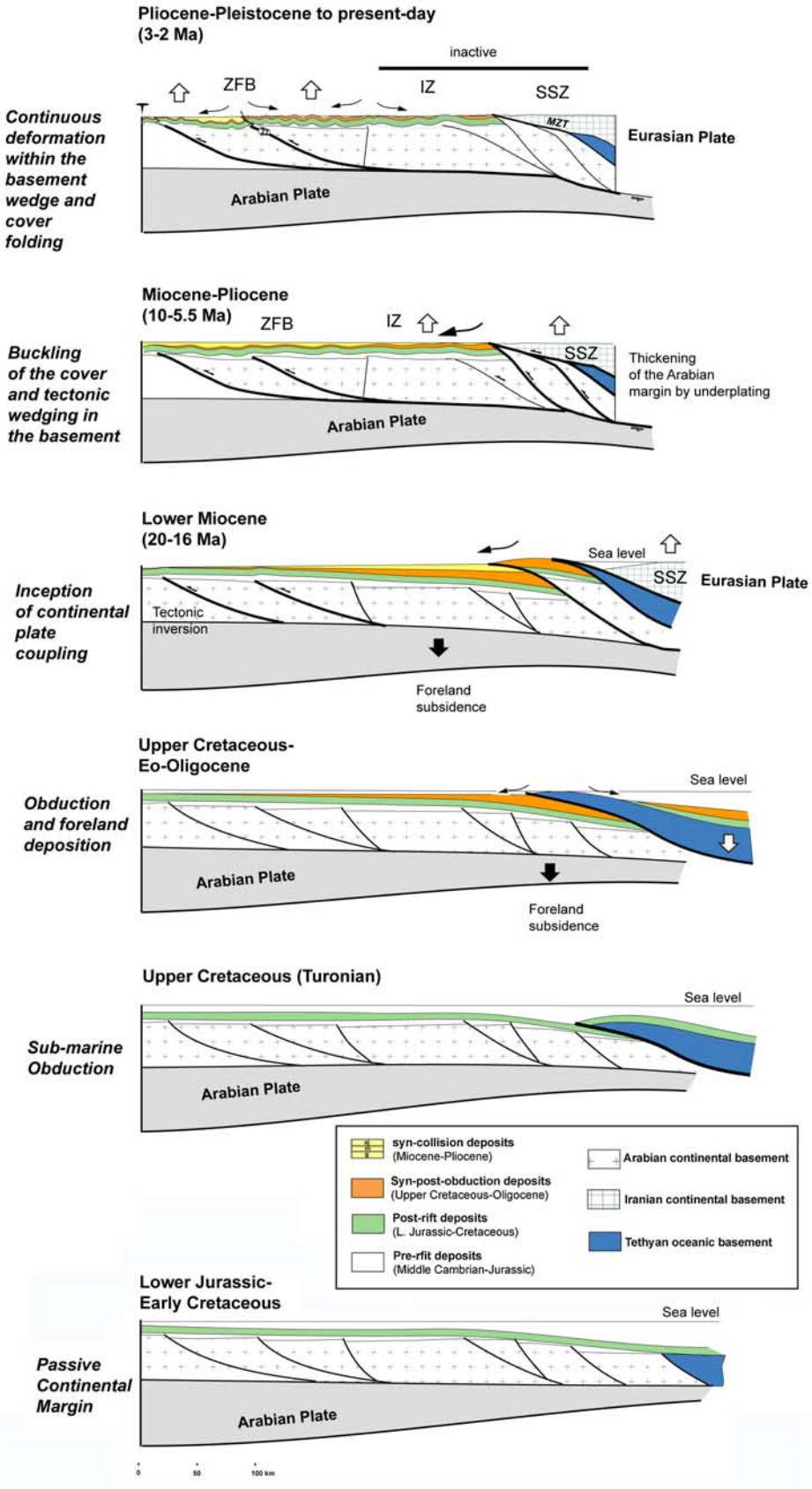
Pliocene-Pleistocene to present-day
(3-2 Ma)
inactive
ZFB
IZ
SSZ
MZT
Eurasian Plate
Continuous deformation within the basement wedge and cover folding
Arabian Plate
Miocene-Pliocene
(10-5.5 Ma)
ZFB
IZ
SSZ
Thickening of the Arabian margin by underplating
Buckling of the cover and tectonic wedging in the basement
Arabian Plate
Lower Miocene
(20-16 Ma)
Sea level
SSZ
Eurasian Plate
Inception of continental plate coupling
Tectonic inversion
Foreland subsidence
Upper Cretaceous-
Eo-Oligocene
Sea level
Obduction and foreland deposition
Arabian Plate
Foreland subsidence
Upper Cretaceous (Turonian)
Sea level
Sub-marine Obduction
Arabian Plate
syn-collision deposits
(Miocene-Pliocene)
Syn-post-obduction deposits
(Upper Cretaceous-Oligocene)
Post-rift deposits
(L. Jurassic-Cretaceous)
Pre-rfit deposits
(Middle Cambrian-Jurassic)
Arabian continental basement
Iranian continental basement
Tethyan oceanic basement
Lower Jurassic-
Early Cretaceous
Sea level
Passive Continental Margin
Arabian Plate
0
50
100 km

Figure 19

trending topographic ridge formed by the stacking of ophiolitic thrust sheets. However, the persistence of early Miocene flyschs in the High Zagros of the Dezful domain (Figure 19) suggests that the closure of the Neo-Tethys might have been not completed before the Miocene [*Stoneley*, 1981]. Post-Asmari clastics form a progradational syn-collisional sequence deposited in the subsident Zagros foreland basin fed by the products of the erosion of the hinterland. This stage is considered by several authors as being controlled by the final closure of the Neo-Tethyan ocean [*Elmore and Farrand*, 1981; *McQuarrie et al.*, 2003].

[61] Basement-involved deformation started ~20–16 Ma (Early Middle Miocene) and predated the initiation of cover folding (Figure 19). This early compressional deformation is related to the onset of plate coupling and intraplate stress buildup released along favorably oriented inherited basement features. Initiation of margin inversion correlates well with the change from a homogeneous and regional carbonate sedimentation of the Asmari and Qom Formations. Margin inversion occurred by the reactivation of a complex array of NW–SE-trending Tethyan normal faults (e.g., Surmeh Fault, Mountain Front Fault) and Panafrican inherited N–S fault trend (Karebass, Sabz-Pushan, Sarvestan transcurrent faults). This early tectonic inversion of basement faults has been also documented northward in the Dezful embayment [*Ahmadhadi et al.*, 2007]. Coevally with intraplate stress buildup, isopachs showed that the Neogene foreland basin developed at that time. We notice that the 200 to 300 km width of the foreland basin (Figure 19) is consistent with flexural wavelength for an elastic plate thickness of 50 km [*Snyder and Barazangi*, 1986]. It is possibly further compatible with buckling of the lithosphere often proposed at an initial stage of collision [*Burg et al.*, 1994; *Cloetingh et al.*, 1999].

[62] The early phase of deformation accommodated little shortening in the basement. As suggested by crustal-scale section of Figure 4, the major part of the basement deformation was achieved by underplating of Arabian upper crustal duplexes beneath the Main Zagros Thrust. In order to be consistent with geodynamical reconstructions [*McQuarrie et al.*, 2003] and the increase of subsidence coeval with the deposition of the Agha Jari Formation (Figure 19) we suggest that underplating and associated thickening of the upper crust occurred ~10 Ma.

[63] The Zagros foreland remained a flexural basin accumulating synorogenic deposits until intraplate stresses uniformly yield the brittle strength of upper crustal rocks, ~5.5 Ma. At this point, the foreland basin evolved into an orogenic belt controlled by the southward propagation of a brittle upper crustal wedge over a ductile lower crust. Reverse movements along inverted basement structures generalized in the upper brittle crust coeval with the initiation of cover folding (buckling). Despite the limited number of available sections, stratigraphic constraints suggest that thin-skinned cover folding developed rapidly all over the Zagros Folded Belt.

[64] Most folds become emergent ~3–2 Ma as attested by alluvial deposits of the Bakhtyari Formation that filled most of the synclinal valleys while the crest of anticlines underwent erosion. Together with basement deformation, which is responsible for the regional uplift, erosion could have promoted folding during the Pleistocene as shown by folded Bakhtyari conglomerates (Figure 19). We estimate that anticlines grew at rates of 0.3–0.6 mm/yr and forced the rivers, with an initially south-flowing course, to flow axially. We further suggest that the Bakhtyari Formation never formed a huge and continuous alluvial fan covering the whole ZFB, otherwise the rivers feeding the fans would have cut through the folds. This supports a local origin for the provenance of sediments, i.e., from folds, within the Bakhtyari Formation. The deformation is still ongoing in the basement as shown by active faulting and it is currently supported in the cover by the tilting of recent terraces and GPS survey [*Walpersdorf et al.*, 2006]. We finally infer that the building of both shallow and deep structural styles was simultaneous in the past 5.5 Ma. The way they deform however is different; the basement is prefractured so it shortens preferentially by faulting. In contrast, the sedimentary cover is more homogenous and thus folding may occur by buckling. However, as strain rates increase during earthquakes stress transfer from basement to cover is possible.

7.3. Sequence of Deformation and Plate Reconstruction: A Key to Climatic and Tectonic Forcing in the Zagros Collision Area

[65] The timing of the onset of siliclastics accumulation in the modern Zagros foreland is well correlated with the reduction of Arabia/Eurasia plate convergence near 25 Ma [*McQuarrie et al.*, 2003] and with the observation that the uplift of the Iranian plateau occurred after the deposition of the marine strata of the Qom Formation, i.e., after the Chattian, 28 Ma ago. Following the opening of the Gulf of Aden [*d'Acremont et al.*, 2006], molassic sediment accumulation increased over the past 10 Ma to reach rates of 182 m/Ma. This is in fairly good agreement with the most recent age proposed for closure of the Tethyan ocean based on plate reconstruction [*McQuarrie et al.*, 2003] and is consistent with the cooling, exhumation and uplift of the west-central Alborz [*Axen et al.*, 2001]. Underplating of Arabian slab units beneath the Sanandaj-Sirjan belt likely occurred at this time. We should further notice that this period is close to both the accepted 8.5 Ma age for the monsoon intensification [e.g., *Molnar et al.*, 1993], and the global cooling event in the middle Miocene ~12–14 Ma recognized in deep ocean water [*Zachos et al.*, 2001]. This would potentially support climatic forcing to be responsible for the observed increased in Upper Miocene sediment accumulation. However, it is not before 5 Ma that the main period of shortening started, allowing for the uplift of the ZFB in association with basement-involved shortening and development of thin-skinned cover folding. This is coeval with the widespread tectonic change at ~5 Ma possibly caused by the Dead Sea transform zone reorganization [*Axen et al.*, 2001] and onset of oceanic spreading in the Red Sea by 3.4 Ma [*Chu and Gordon*, 1998].

[66] Given the age of the onset of the main phase of deformation that occurred in the past 10 Ma, we deduce that the Zagros collision accommodated shortening rates of 6.5–

8 km/Ma. This amount is comparable with present-day rate of 7 mm/yr deduced from GPS data [*Vernant et al.*, 2004]. The local tilting of Quaternary terraces observed near the mountain front [e.g., *Mann and Vita-Finzi*, 1988] and deformation patterns pictured by GPS data [*Walpersdorf et al.*, 2006] as well as ^{14}C dating of Holocene fluvio-marine terraces [*Oveisi et al.*, 2007] show that 35% to 50% of the convergence is currently accommodated at the Mountain Front.

8. Conclusions

[67] The observations of dominant fold wavelengths (15.8 ± 5.3 km) in the Fars, stratigraphic constraints on synfolding/postfolding strata, drainage network organization together with the homogeneous differential stresses (40 ± 15 MPa) across the Zagros point to buckling as the first-order process responsible for fold development whereas the basement shortens preferentially by reverse/strike-slip faulting. The sequence of cover versus basement deformation can be drawn as follows.

[68] 1. The first stage of deformation in the Zagros foreland basin occurred in the early Miocene ~20 Ma prior to cover folding and refers to the inversion of the Arabian margin. This conveys the onset of plate coupling and buildup of intraplate stresses which is consistent with the reduction of the Arabia/Eurasian plate convergence [*McQuarrie et al.*, 2003]. The early Miocene times further coincide with the onset of accumulation of Neogene siliciclastics (Fars Group) in the foreland. By Middle-Upper Miocene, ~10 Ma, contraction increased drastically in relation with underplating of Arabian crustal units beneath the Sanandaj-Sirjan zone. This event is recorded by the increase of sedimentation rates up to 182 m/Ma. Monsoon intensification in the region [*Molnar et al.*, 1993] and global cooling [*Zachos et al.*, 2001] might have also contributed to increased erosion without requiring any important surface uplift.

[69] 2. It is not before 5 Ma that basement deformation produced the southward propagation of the basement wedge and regional uplift of the Zagros. At the same time, shortening in the cover started by buckling. As crustal shortening increased, folding developed through detachment folds growing by limb rotation as revealed by growth strata of the Agha Jari Formation. Ongoing contraction and erosion finally led to the rejuvenation of folds ~3–2 Ma with uplift rates of the order of 0.3–0.6 mm/yr which forced the rivers to flow axially.

[70] 3. On the basis of a new crustal-scale section, we estimate a total shortening of 65–78 km across the Zagros Mountains. Only a small amount, i.e., 15 km, was accommodated across the ZFB in both the cover and the basement. In contrast, more than 75% of shortening was taken up by underplating of the Arabian basement beneath the Iranian plate. We deduce that the Zagros collision accommodated shortening rates of 6.5–8 km/Ma in the past 10 Ma This amount is comparable with present-day rates of ~7 mm/yr proposed from geodetic surveys [*Vernant et al.*, 2004].

[71] Such a study of long-term deformation on the northern margin of the Arabian plate, in the Zagros Folded Belt, provides insights on how plate boundary forces in collisional setting are transmitted and distributed within the continental lithosphere. Specifically we pointed out that even though thin-skinned deformation in the sedimentary cover may be spectacular important in collisional fold-thrust belts like the Zagros Folded Belt, basement-involved or deep crustal deformation should not be neglected as it requires far less shortening than equivalent thin-skinned models do.

[72] **Acknowledgments.** This work has been supported by the Middle East Basin Evolution (MEBE) program. The authors are indebted to the Geological Survey of Iran for its support for fieldwork and especially A. Saidi and P. Navabpour. The authors would like to thank G. Bertotti and an anonymous reviewer for their constructive review as well as S. Castelltort and L. Dissez for their help and suggestions during the writing of the article.

References

Ahmadhadi, F., O. Lacombe, and J.-M. Daniel (2007), Early reactivation of basement faults in Central Zagros (SW Iran): Evidence from pre-folding fracture populations in Asmari Formation and Lower Tertiary paleogeography, in *Thrust Belts and Foreland Basins: From Fold Kinematics to Hydrocarbon Systems*, edited by O. Lacombe et al. pp. 205–228, Springer, New York.

Alvarez, W. (1999), Drainage on evolving fold-thrust belts: A study of transverse canyons in the Apennines, *Basin Res.*, *11*, 267–284.

Ambraseys, N. N., and C. P. Melville (1982), *A History of Persian Earthquakes*, Cambridge Univ. Press, Cambridge, U. K.

Amrouch, K., O. Lacombe, F. Mouthereau, and L. Dissez (2005), Quantification of orientations and magnitudes of the late Cenozoic paleostresses in the Zagros folded belt from calcite twin analysis, paper presented at Thrust Belts and Foreland Basins: International Meeting, Soc. Geol. de France, Rueil-Malmaison, France.

Axen, G., P. S. Lam, M. Grove, D. F. Stockli, and J. Hassanzadeh (2001), Exhumation of the west-central Alborz Mountains, Iran, Caspian subsidence, and collision-related tectonics, *Geology*, *29*, 559–562.

Bahroudi, A., and H. A. Koyi (2003), Effect of spatial distribution of Hormuz salt on deformation style in the Zagros fold and thrust belt: An analogue modelling approach, *J. Geol. Soc.*, *160*, 1–15.

Berberian, M. (1995), Master "blind" thrust faults hidden under the Zagros folds: Active basement tectonics and surface tectonics surface morphotectonics, *Tectonophysics*, *241*, 193–224.

Beydoun, Z. R., M. W. H. Clarke, and R. Stoneley (1992), Petroleum in the Zagros Basin: A late Tertiary foreland basin overprinted onto the outer edge of a vast hydrocarbon-rich Paleozoic-Mesozoic passive-margin shelf, in *Foreland Basins and Fold Belts*, *AAPG Mem.*, vol. 55, edited by R. W. Macqueen and D. A. Leckie, pp. 309–339, Am. Assoc. of Petrol. Geol., Tulsa, Okla.

Biot, M. A. (1961), Theory of folding of stratified viscoelastic media and its implications in tectonics and orogenesis, *Geol. Soc. Am. Bull.*, *72*, 1595–1620.

Blanc, E. J.-P., M. B. Allen, S. Inger, and H. Hassani (2003), Structural styles in the Zagros simple folded zone, Iran, *J. Geol. Soc.*, *160*, 401–412.

Burbank, D. W., A. J. Meigs, and N. Brozovic (1996), Interactions of growing folds and coeval depositional systems, *Basin Res.*, *8*, 199–223.

Burg, J. P., P. Davy, and J. Martinod (1994), Shortening of analogue models of the continental lithosphere: New hypothesis for the formation of the Tibetan plateau, *Tectonics*, *13*, 475–483.

Burov, E. B., and M. Diament (1995), The effective elastic thickness (T_e) of continental lithosphere: What does it really mean?, *J. Geophys. Res.*, *100*, 3905–3927.

Butler, R. W. H., et al. (2004), Applying thick-skinned tectonic models to the Apennine thrust belt of Italy—Limitations and Implications, in *Thrust Tectonics and Hydrocarbon Systems*, *AAPG Mem.*, vol. 82, edited by K. R. McClay, pp. 647-667, Am. Assoc. of Petrol. Geol., Tulsa, Okla.

Chu, D., and R. G. Gordon (1998), Current plate motions across the Red Sea, *Geophys. J. Int.*, *135*, 313–328.

Cloetingh, S., E. Burov, and A. Poliakov (1999), Lithosphere folding: Primary response to compression ? (from central Asia to Paris basin), *Tectonics*, *18*, 1064–1083.

Colman-Sadd, S. (1978), Fold development in Zagros simply folded belt, Southwest Iran, *Am. Assoc. Pet. Geol. Bull.*, *62*, 984–1003.

Costa, E., and B. C. Vendeville (2002), Experimental insights on the geometry and kinematics of fold-and-thrust belts above weak, viscous evaporitic décollement, *J. Struct. Geol.*, *24*, 1729–1739.

Coward, M. P., M. De Donatis, S. Mazzoli, W. Paltrinieri, and F.-C. Wezel (1999), Frontal part of the northern Apennines fold and thrust belt in the Romagna-Marche area (Italy): Shallow and deep structural styles, *Tectonics*, *18*, 559–574.

Cristallini, E. O., and V. A. Ramos (2000), Thick-skinned and thin-skinned thrusting in the La Ramada fold and thrust belt: Crustal evolution of the High Andes of San Juan, Argentina (32°SL), *Tectonophysics*, *317*, 205–235.

d'Acremont, E., S. Leroy, M. Maia, P. Patriat, M.-O. Beslier, N. Bellahsen, M. Fournier, and P. Gente (2006), Structure and evolution of the eastern Gulf of Aden: Insights from magnetic and gravity data (Encens-Sheba MD117 cruise), *Geophys. J. Int.*, *165*, 786–803.

Davis, D. M., and T. Engelder (1985), Role of salt in fold-and-thrust belts, *Tectonophysics*, *119*, 67–88.

De Mets, C., R. G. Gordon, D. F. Argus, and S. Stein (1994), Effects of recent revision to the geomagnetic reversal time scale on estimates of current plate motions, *Geophys. Res. Lett.*, *21*, 2191–2194.

Elmore, R. D., and W. R. Farrand (1981), Asphalt-bearing sediment in synorogenic Miocene-Pliocene molasse, Zagros Mountains, Iran, *Am. Assoc. Pet. Geol. Bull.*, *65*, 1160–1165.

Falcon, N. (1974), Zagros Mountains, Mesozoic-Cenozoic orogenic belts, *Geol. Soc. Spec. Publ.*, *4*, 199–211.

Ford, M., E. A. Williams, A. Artoni, J. Vergès, and S. Hardy (1996), Progressive evolution of a fault-related fold pair from growth strata geometries, Sant Llorenç de Morunys, SE Pyrenees, *J. Struct. Geol.*, *19*, 413–441.

Haq, B. U., J. Hardenbol, and P. R. Vail (1987), Chronology of fluctuating sea-levels since the Triassic, *Science*, *235*, 1156–1167.

Hatzfeld, D., M. Tatar, K. Priestley, and M. Ghafori-Ashtiany (2003), Seismological constraints on the crustal structure beneath the Zagros Mountain Belt (Iran), *Geophys. J. Int.*, *155*, 403–410.

Hempton, M. R. (1987), Constraints on Arabian Plate motion and extensional history of the Red Sea, *Tectonics*, *6*, 687–705.

Hessami, K., H. A. Koyi, C. J. Talbot, H. Tabasi, and E. Shabanian (2001), Progressive unconformities within an evolving foreland fold-thrust belt, Zagros Mountains, *J. Geol. Soc.*, *158*, 969–981.

Homke, S., J. Verges, G. Garces, H. Emamia, and R. Karpuzc (2004), Magnetostratigraphy of Miocene-Pliocene Zagros foreland deposits in the front of the Push-e Kush Arc (Lurestan Province, Iran), *Earth Planet. Sci. Lett.*, *225*, 397–410.

Homke, S., J. Verges, J. Serra-Kiel, G. Bernaola, G. Miguel, I. M. Verdu, I. Sharp, R. Karpuz, and M. Goodarzi (2007), Formation of the early Zagros foreland basin: biostratigraphic and magnetostratigraphic evidence from the Paleocene Amiran, Taleh Zang and Kashkan formations of Lurestan Province, SW Iran, *Geol. Soc. Am. Bull.*, in press.

Jackson, J. A. (1980), Reactivation of basement faults and crustal shortening in orogenic belts, *Nature*, *283*, 343–346.

Jackson, J. A., and D. McKenzie (1988), The relationship between plate motions and seismic moments tensors and the rates of active deformation in the Mediterranean and Middle East, *Geophys. J. Int.*, *83*, 45–73.

James, G. A., and J. G. Wynd (1965), Stratigraphic nomenclature of Iranian oil consortium agreement area, *Am. Assoc. Pet. Geol. Bull.*, *49*, 2162–2245.

Jaumé, S. C., and R. J. Lillie (1988), Mechanics of the Salt Range-Potwar Plateau, Pakistan: A fold-and-thrust belt underlain by evaporites, *Tectonics*, *7*, 57–71.

Koop, W., and R. Stoneley (1982), Subsidence history of the middle East Zagros basin, Permian to Recent, *Philos. Trans. R. Soc., Ser. A*, *305*, 149–168.

Lacombe, O., and F. Mouthereau (2002), Basement-involved shortening and deep detachment tectonics in forelands of orogens: Insights from recent collision belts (Taiwan, Western Alps, Pyrenees), *Tectonics*, *21*(4), 1030, doi:10.1029/2001TC901018.

Lacombe, O., F. Mouthereau, S. Kargar, and B. Meyer (2006), Late Cenozoic and modern stress fields in the western Fars (Iran): Implications for the tectonic and kinematic evolution of central Zagros, *Tectonics*, *25*, TC1003, doi:10.1029/2005TC001831.

Lacombe, O., K. Amrouch, F. Mouthereau, and L. Dissez (2007), Calcite twinning constraints on late Neogene stress patterns and deformation mechanisms in the active Zagros collision belt, *Geology*, *35*, 263–266.

Lee, C.-I., Y.-L. Chang, and M. P. Coward (2002), Inversion tectonics of the fold-and-thrust belt, western Taiwan, in *Geology and Geophysics of an Arc-Continent Collision, Taiwan*, edited by T. B. Byrne and C.-S. Liu, *Spec. Pap. Geol. Soc.*, *358*, 13-30.

Mann, C. D., and C. Vita-Finzi (1988) Holocene serial folding in the Zagros, in *Gondwana and Tethys*, edited by M. G. Audley-Charles and A. Hallam, *Geol. Soc. Spec. Publ.*, *37*, 51-59.

Masson, F., J. Chéry, D. Hatzfeld, J. Martinod, P. Vernant, F. Tavakoli, and M. Ghafory-Ashtiani (2004), Seismic versus aseismic deformation in Iran inferred from earthquakes and geodetic data, *Geophys. J. Int.*, *160*, 217–226.

McQuarrie, N. (2004), Crustal scale geometry of the Zagros fold-thrust belt, Iran, *J. Struct. Geol.*, *26*, 519–535.

McQuarrie, N., J. M. Stock, C. Verdel, and B. P. Wernicke (2003), Cenozoic evolution of Neotethys and implications for the causes of plate motions, *Geophys. Res. Lett.*, *30*(20), 2036, doi:10.1029/2003GL017992.

Meyer, B., R. Lacassin, J. Brulhet, and B. Mouroux (1994), The Basel 1356 earthquake: Which fault produced it?, *Terra Nova*, *6*, 54–63.

Molinaro, M., P. Leturmy, J.-C. Guezou, D. Frizon de Lamotte, and S. A. Eshraghi (2005), The structure and kinematics of the south-eastern Zagros fold-thrust belt; Iran: From thin-skinned to thick-skinned tectonics, *Tectonics*, *24*, TC3007, doi:10.1029/2004TC001633.

Molnar, P., P. England, and J. Martinod (1993), Mantle dynamics, uplift of the Tibetan plateau, and the Indian monsoon, *Rev. Geophys.*, *31*, 357–396.

Motiei, H. (1993), *Geology of Iran: Stratigraphy of Zagros*, 536 pp., Geol. Surv. of Iran, Tehran.

Mouthereau, F., and O. Lacombe (2006), Inversion of the Paleogene Chinese continental margin and thick-skinned deformation in the Western Foreland of Taiwan, *J. Struct. Geol.*, *28*, 1977–1993.

Mouthereau, F., O. Lacombe, and B. Meyer (2006), The Zagros Folded Belt (Fars, Iran): Constraints from topography and critical wedge modelling, *Geophys. J. Int.*, *165*, 336–356.

Mouthereau, F., O. Lacombe, J. Tensi, N. Bellahsen, S. Kargar, and K. Amrouch (2007), Mechanical constraints on the development of The Zagros Folded Belt (Fars), in *Thrust Belts and Foreland Basins: From Fold Kinematics to Hydrocarbon Systems*, edited by O. Lacombe et al., pp. 245-264, Springer, New York.

National Iranian Oil Company (1977), Geological map of Iran, sheet 5, South-central Iran, Tehran.

Ni, J., and M. Barazangi (1986), Seismotectonics of the Zagros continental collision zone and a comparison with the Himilayas, *J. Geophys. Res.*, *91*, 8205–8218.

Oberlander, T. (1985), Origin of drainage transverse to structures in orogens, in *Tectonic Geomorphology*, edited by J. Hack and M. Morisawa, pp. 155-182, Allen and Unwin, Boston, Mass.

Oveisi, B., J. Lavé, and P. Van der Beek (2007), Active folding and deformation rate at the central Zagros front (Iran), in *Thrust Belts and Foreland Basins: From Fold Kinematics to Hydrocarbon Systems*, edited by O. Lacombe et al., pp. 267-287, Springer, New York.

Paul, A., A. Kaviani, D. Hatzfeld, J. Vergne, and M. Mokhtari (2006), Seismological evidence for crustal-scale thrusting in the Zagros mountain belt (Iran), *Geophys. J. Int.*, *166*, 227–237.

Rostein, Y., and M. Schaming (2004), Seismic reflection evidence for thick-skinned tectonics in the northern Jura, *Terra Nova*, *16*, 250–256.

Sans, M., J. Verges, E. Gomis, J. M. Parès, M. Schiattarella, A. Travé, F. Calvet, P. Santanach, and A. Doulcet (2003), Layer parallel shortening in salt-detached folds: Constraint on cross-section restoration, *Tectonophysics*, *372*, 85–104.

Schmalholz, S. M., Y. Podladchikov, and J. P. Burg (2002), Control of folding by gravity and matrix thickness: Implications for large-scale folding, *J. Geophys. Res.*, *107*(B1), 2005, doi:10.1029/2001JB000355.

Schuster, F., and U. Wielandt (1999), Oligocene and early Miocene coral faunas from Iran: Palaeoecology and palaeobiogeography, *Int. J. Earth Sci.*, *88*, 571–581.

Sherkati, S., and J. Letouzey (2004), Variation of structural style and basin evolution in the central Zagros (Izeh zone and Dezful Embayment), Iran, *Mar. Pet. Geol.*, *21*, 535–554.

Sherkati, S., M. Molinaro, D. Frizon de Lamotte, and J. Letouzey (2005), Detachment folding in the Central and Eastern Zagros fold-belt (Iran): Salt mobility, multiple detachments and late basement control, *J. Struct. Geol.*, *27*, 1680–1696.

Sinclair, H. D. (1997), Tectonostratigraphic model for underfilled peripheral basins: An Alpine perspective, *Geol. Soc. Am. Bull.*, *109*, 324–346.

Smit, J. H. W., J. P. Brun, and D. Sokoutis (2003), Deformation of brittle-ductile thrust wedges in experiments and nature, *J. Geophys. Res.*, *108*(B10), 2480, doi:10.1029/2002JB002190.

Snyder, D. B., and M. Barazangi (1986), Deep crustal structure and flexure of the Arabian plate beneath the Zagros collisional mountain belt as inferred from gravity observations, *Tectonics*, *5*, 361–373.

Sommaruga, A. (1999), Décollement tectonics in the Jura foreland fold-and thrust belt, *Mar. Pet. Geol.*, *16*, 111–134.

Stocklin, J. (1968), Structural history and tectonics of Iran; a review, *Am. Assoc. Pet. Geol. Bull.*, *52*, 1229–1258.

Stoneley, R. (1981), The geology of the Kuh-e Dalneshin area of southern Iran, and its bearing on the evolution of southern Tethys, *J. Geol. Soc.*, *138*, 509–526.

Stoneley, R. (1990), The Arabian continental margin in Iran during the Late Cretaceous, in *The Geology and Tectonics of the Oman Region*, edited by A. H. F. Robertson, M. P. Searle, and A. C. Ries, pp. 787–795, Geol. Soc., London.

Storti, F., and K. McClay (1995), Influence of syntectonic sedimentation on thrust wedges in analogue models, *Geology*, *23*, 999–1002.

Talbot, C. J., and M. Alavi (1996), The past of a future syntaxis across the Zagros, in Alsop, in *Salt Tectonics*, edited by G. I. Alsop, D. J. Blundell, and I. Davison, *Geol Soc Am. Spec. Pap.*, *100*, 89-109.

Talebian, M., and J. A. Jackson (2004), A reappraisal of earthquake focal mechanisms and active shortening in the Zagros mountains of Iran, *Geophys. J. Int.*, *156*, 506–526.

Tatar, M., D. Hatzfeld, and M. Ghafori-Ashtiany (2004), Tectonics of the Central Zagros (Iran) deduced from microearthquakes seismicity, *Geophys. J. Int.*, *156*, 255–266.

Tucker, G. E., and R. Slingerland (1996), Predicting sediment flux from fold and thrust belts, *Basin Res.*, *8*, 329–349.

Tucker, M. E. (2005), *Sedimentary Petrology: An Introduction to the Origin of Sedimentary Rocks*, 262 pp., Blackwell, Oxford, U. K.

Turcotte, D. L., and G. Schubert (2002), *Geodynamics: Applications of Continuum Mechanics to Geological Problems*, Cambridge Univ. Press, Cambridge, U. K.

Vernant, P., et al. (2004), Present-day crustal deformation and plate kinematics in the Middle East constrained by GPS measurements in Iran and northern Oman, *Geophys. J. Int.*, *157*, 381–398.

Walpersdorf, A., D. Hatzfeld, H. Nankali, F. Tavakoli, F. Nilforoushan, M. Tatar, P. Vernant, J. Chery, and F. Masson (2006), Difference in the GPS deformation pattern of North and Central Zagros (Iran), *Geophys. J. Int.*, *167*, 1077–1088.

Watts, A. B. (2001), *Isostasy and Flexure of the Lithosphere*, Cambridge Univ. Press, Cambridge, U.K.

Zachos, J., M. Pagani, L. Sloan, E. Thomas, and K. Billups (2001), Trends, rhythms, and aberrations in global climate 65 Ma to present, *Science*, *292*, 686–693, doi:10.1126/science.1059412.

Zapata, T. R., and R. W. Allmendinger (1996), Thrust-front zone of the Precordillera, Argentina: A thick-skinned triangle zone, *Am. Assoc. Pet. Geol. Bull.*, *80*, 359–381.

Zhang, Y., B. E. Hobbs, A. Ord, and H. B. Mühlhaus (1996), Computer simulation of single-layer buckling, *J. Struct. Geol.*, *18*, 643–655.

Ziegler, M. A. (2001), Late Permian to Holocene paleofacies evolution of the Arabian Plate and its hydrocarbon occurrences, *GeoArabia*, *6*, 445–503.

N. Bellahsen, T. De Boisgrollier, O. Lacombe, F. Mouthereau, and J. Tensi, Laboratoire Tectonique, Université Pierre et Marie Curie, UMR 7072, 75252, Paris Cedex05, France. (bellah@ccr.jusieu.fr; thomas.deboisgrollier@lgs.jussieu.fr; olacombe@ccr.jussieu.fr; frederic.mouther@ccr.jussieu.fr; julien.tensi@lgs.jussieu.fr)

S. Kargar, Geological Survey of Iran, Meraj Avenue, Azadi Square, Tehran 13185-1494, Iran. (shahram_kargar_geo@yahoo.com)